Hyperbranched Polytriazoles: Click Polymerization, Regioisomeric Structure, Light Emission, and Fluorescent Patterning

Anjun Qin,[†] Jacky W. Y. Lam,[†] Cathy K. W. Jim,[†] Li Zhang,[†] Jingjing Yan,[‡] Matthias Häussler,[†] Jianzhao Liu,[†] Yongqiang Dong,[†] Dehai Liang,[‡] Erqiang Chen,[‡] Guochen Jia,[†] and Ben Zhong Tang*[,†,§]

Department of Chemistry, The Hong Kong University of Science & Technology, Clear Water Bay, Kowloon, Hong Kong, China; Department of Polymer Science and Engineering, Peking University, Beijing 100871, China; and Department of Polymer Science & Engineering, Zhejiang University, Hangzhou 310027, China

Received March 10, 2008

ABSTRACT: Synthesis of hyperbranched poly(1,2,3-triazole)s (*hb*-PTAs) has been a challenge: the AB_2 monomers were inclined to self-oligomerize, and their Cu(I)-catalyzed click polymerizations failed to yield soluble polymers. We tackled the challenge in this work and succeeded in generating *hb*-PTAs with regioregularity, processability, and functionality. We took an $A_2 + B_3$ approach and used diazides **2** and triyne **3** as monomers, which are free of self-oligomerization concerns. Thermal polymerizations of **2** and **3** produced regiorandom polymers (*hb-r*-P**1**) with high molecular weights in high yields. Metal-mediated regioselective polymerizations afforded soluble 1,4- and 1,5-linked polymers (*hb*-1,4-P**1** and *hb*-1,5-P**1**), presenting the first examples of regioregular *hb*-PTAs with macroscopic processability. The reactions were affected by substrate and catalyst: electron-rich alkyne generally slowed down the cycloaddition reaction, while ruthenium catalysts ($Cp^*Ru(PPh_3)_2Cl$ and $[Cp^*RuCl_2]_n$) exhibited higher substrate tolerance than copper catalyst [$Cu(PPh_3)_3Br$]. Regiostructures and regioregularities of the *hb*-PTAs were determined spectroscopically. Degrees of branching of *hb-r*-P**1** were calculated to be ∼90%. Conformations of the *hb*-PTAs were affected by the steric effects between their aromatic units, which in turn affected their solubility, conjugation, luminescence, and aggregation. While the polymer solutions all emitted deep blue light, the films of *hb*-1,4-P**1**, *hb*-1,5-P**1** and *hb-r*-P**1** emitted blue, yellow, and white light, respectively, due to the difference in the aggregation of their chromophoric units in the solid state. Fluorescent photoresist patterns with various emission colors were readily generated from photo-cross-linking of the polymers through a nitrene-mediated photolysis mechanism.

Introduction

Chemists have worked enthusiastically toward the development of new reactions with efficient atom economy, strong functionality tolerance, and high stereo- and regioselectivity. A remarkable progress along this line has been the development of "click chemistry"[1,2] for effective and selective chemical transformations. A "click reaction" can create functional molecules with heteroatom links from reactive modular building blocks in high efficiency under benign conditions through simple isolation procedures. A number of click reactions have been explored and identified, with the metal-catalyzed Huisgen [3 + 2] azide−alkyne cycloaddition[3] being hailed as the cream of the crop. The Cu(I)- and Ru(II)-mediated 1,3-dipolar cycloadditions proceed steadily, affording 1,4- and 1,5-disubstituted 1,2,3-triazoles, respectively, in high yields.[1,2]

The azide−alkyne click reaction is modular, regioselective, and efficient and requires mild reaction conditions and simple purification procedures. These appealing features have enabled the reaction to evolve into a powerful synthetic tool, finding applications in diverse areas including drug discovery, bioconjugate chemistry, surface modification, and materials development.[2,4] The click reaction has also been utilized in polymer science, mainly in the area of functionalization of preformed polymers through postpolymerization reactions.[5,6] The azido- and ethynyl-functionalized polymers have been used as the branching points and chain extenders for the syntheses of graft and block copolymers, respectively. Taking the click reaction-based "graft-to" and "graft-from" approaches, linear polymer chains decorated by dendritic grafts (or dendronized linear polymers) have been successfully prepared.[6,7]

Synthetic polymer chemists have attempted to develop the click reaction into a new polymerization technique. The effort, however, has met with limited success. The Cu(I)-catalyzed polymerizations of arylenediazides (N_3-Ar-N_3) and arylenediynes ($HC\equiv C-Ar-C\equiv H$) (Ar = phenyl, pyridyl, fluorenyl, etc.) were sluggish, taking as long as 7−10 days to finish.[8] The products often precipitated from the reaction mixtures even at the oligomer stage or became insoluble in common organic solvents after purification, unless very long alkyl chains, such as *n*-dodecyl groups, were attached to the arylene rings. All the polymers were nonfluorescent in the solid state, although their dilute solutions emitted UV light, suggesting that the polymer luminescence was quenched by aggregate formation.

Triazole dendrimers have been elegantly synthesized from the Cu(I)-catalyzed ligation of azides and alkynes.[9] Notwithstanding the powerfulness of click reaction, it still takes about 10 steps to prepare a dendrimer comprising of third-generation dendrons with an absolute molecular weight of about 6000. Hyperbranched polymer is a structural congener of dendritic polymer. Although structurally imperfect, a hyperbranched polymer can be facilely synthesized via a single-step reaction by a one-pot procedure in large scale and quantity.[10] To explore the utility of click reaction in the synthesis of hyperbranched polymers, two AB_2-type monomers of azidoarylenediynes with a general formula of $N_3-Ar-(C\equiv CH)_2$ have been prepared by two groups in Germany and Belgium.[11] One of the monomers was subjected to Cu(I)-catalyzed polymerization, but the product soon "precipitated" from the reaction mixture, "which is no

* To whom correspondence should be address: Ph +852-2358-7375; Fax +852-2358-1594; e-mail tangbenz@ust.hk.
† The Hong Kong University of Science & Technology.
‡ Peking University.
§ Zhejiang University.

10.1021/ma800538m CCC: $40.75
Published on Web 05/15/2008

Scheme 1. Syntheses of *hb*-PTAs by Metal-Catalyzed Click Polymerizations and Thermally Activated 1,3-Dipolar Polycycloadditions of Diazide (A_2) and Triyne (B_3) Monomers

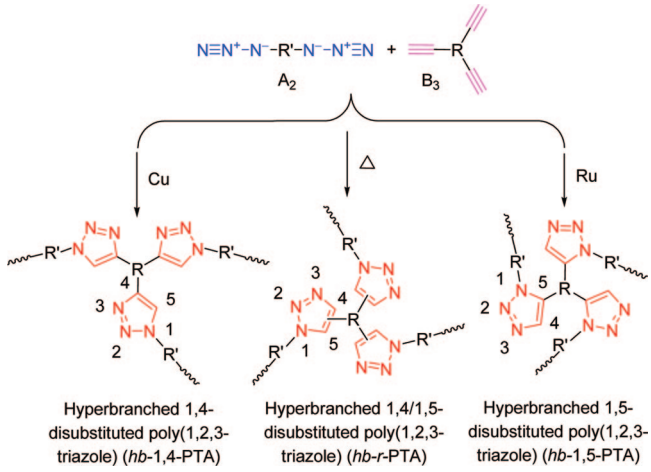

longer soluble in any organic solvent".[11] AB_2-type monomers of ethynylenediazides ($N_3-R-C\equiv C-R-N_3$) have also been prepared. The internal alkyne monomers, however, could only be polymerized by thermally activated 1,3-dipolar polycycloaddition, producing hyperbranched regiorandom poly(1,2,3-triazole)s (*hb-r*-PTAs). In addition, the AB_2 monomers were difficult to prepare and purify and suffered from self-oligomerization during storage under ambient conditions.[11]

Our research groups have been interested in the exploration of alkyne-based polymerization reactions, with the aim of developing alkyne monomers into versatile building blocks for the construction of new macromolecules with linear and hyperbranched structures and advanced functional properties. Using monoynes ($RC\equiv CH$), diynes [$R(C\equiv CH)_2$] and triynes [$R(C\equiv CH)_3$] as monomers, we have successfully synthesized a variety of polyacetylenes, polyarylenes, and polydiynes by metathesis, cyclotrimerization, and coupling polymerizations, respectively.[12] Because of the key role of alkynes in the click reactions and as a natural extension of our alkyne-based research program, we have recently embarked on the syntheses of functional PTAs by click polymerizations.

In our previous work, we have developed a metal-free, thermally initiated, regioselective 1,3-dipolar polycycloaddition process: simply heating a mixture of bis(aroylacetylene) ($HC\equiv C-OArCO-C\equiv CH$) and diazide ($N_3-R-N_3$) in a polar solvent, such as a *N,N*-dimethylformamide (DMF)/toluene mixture, readily furnished a linear PTA with a high regioregularity (1,4-content or $F_{1,4}$ ratio up to ~92%) in a high yield (up to ~98%).[13] In this work, we intended to synthesize hyperbranched polymers (*hb*-PTAs) by click polymerization. We took an $A_2 + B_3$ approach, using easy-to-make and stable-to-keep diazide (A_2) and triyne (B_3) as monomers, in an effort to circumvent the self-oligomerization problem met by the AB_2 systems discussed above. The A_2/B_3 monomers were readily polymerized by metal-mediated click reactions and thermally activated Huigen cycloaddition (Scheme 1). The Cu- and Ru-catalyzed click polymerizations afforded hyperbranched polymers with regular 1,4- and 1,5-linkages (*hb*-1,4- and -1,5-PTAs), respectively. Both polymers are soluble in common solvents, such as dichloromethane (DCM), tetrahydrofuran (THF), and dimethyl sulfoxide (DMSO), representing the first examples of *hb*-PTAs with regioregular structures and macroscopically processability. The steric interactions between the aromatic phenyl and triazole rings affected the electronic communications in the *hb*-PTAs, which in turn influenced their packing and luminescence behaviors in the solid state. Fluorescent images

Scheme 2. Preparation of Diazide Monomers (2)

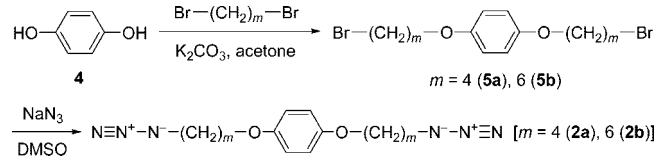

Scheme 3. Preparation of Monoazide Model Compounds (8)

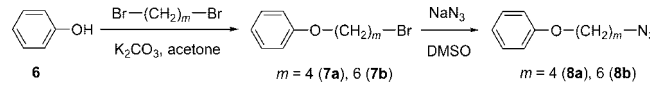

with different emission colors were readily generated by UV photolysis of the polymer films.

Results and Discussion

Monomer Syntheses and Model Reactions. A_2- and B_3-type monomers of diazides **2** and triyne **3** were designed to realize the planned $A_2 + B_3$ approach to *hb*-PTAs. Taking into consideration that click polymerizations of diazide and diyne monomers with rigid structures were inclined to produce insoluble gels,[8] flexible alkyl chains were introduced into the molecular structures of the diazide monomers. The azides, namely 1,4-bis(*n*-azidoalkoxy)benzenes, were facilely prepared by etherization of hydroquinone **4** with α,ω-dibromoalkanes in a basic medium, followed by substitution reaction with sodium azide in DMSO (Scheme 2).

Triphenylamine has been widely used in the development of new organic light-emitting materials and devices due to its excellent solubility and stability as well as high luminescence and hole-transporting efficiencies.[14] Synthetically, it can be readily transformed to a triyne with each of its aryl ring carrying one triple bond at the para position. In this work, we chose triphenylamine as a building block to prepare an amine-cored triyne (B_3) monomer of tris(4-ethynylphenyl)amine (**3**), from which *hb*-PTAs with useful photonic properties may be derived. The monomer was prepared in a high yield (~90%) by iodination of triphenylamine, followed by coupling with (trimethylsilyl)acetylene and base-catalyzed disilylation.[14f,15]

As mentioned above, triphenylamine is a photoresponsive molecule. The amine-cored triyne **3**, however, may show low reactivity toward diazides **2** because of its electron-rich nature. To address this concern, cycloadditions of triyne **3** with monoazides **8** were conducted as model reactions. The monoazides were prepared by the same synthetic routes as the diazides **2**, using phenol **6**, instead of hydroquinone **8**, as a staring material (Scheme 3).

The aminotriyne **3** was subjected to the reaction with monoazides **8** in the presence of the copper catalyst under the standard click reaction conditions[1] (Scheme 4). 1,4-Disubstituted 1,2,3-triazoles **9** were isolated in ~38−54% yields, indicative of a moderate reactivity of triyne **3** in the Cu(I)-catalyzed reaction. The click reactions catalyzed by $Cp^*Ru(PPh_3)_2Cl$, however, produced 1,5-disubstituted 1,2,3-triazoles **10** in higher yields (~79−84%), revealing a higher substrate tolerance of the Ru(II) complex over the Cu(I) catalyst. The model reactions confirm that triyne **3** can be used as a B_3 monomer in the planned $A_2 + B_3$ approach to *hb*-PTAs. An added bonus of these reactions is the provision of model compounds **9** and **10** as authentic standards of 1,4- and 1,5-disubstituted 1,2,3-triazoles for the structural characterization, especially regioregularity elucidation, of the polymer products (*hb*-PTAs) that will be synthesized by the polycycloadditions of triyne **3** with diazides **2** (vide post).

Scheme 4. Syntheses of Model Compounds of 1,4- and 1,5-Disubstituted 1,2,3-Triazoles 9 and 10

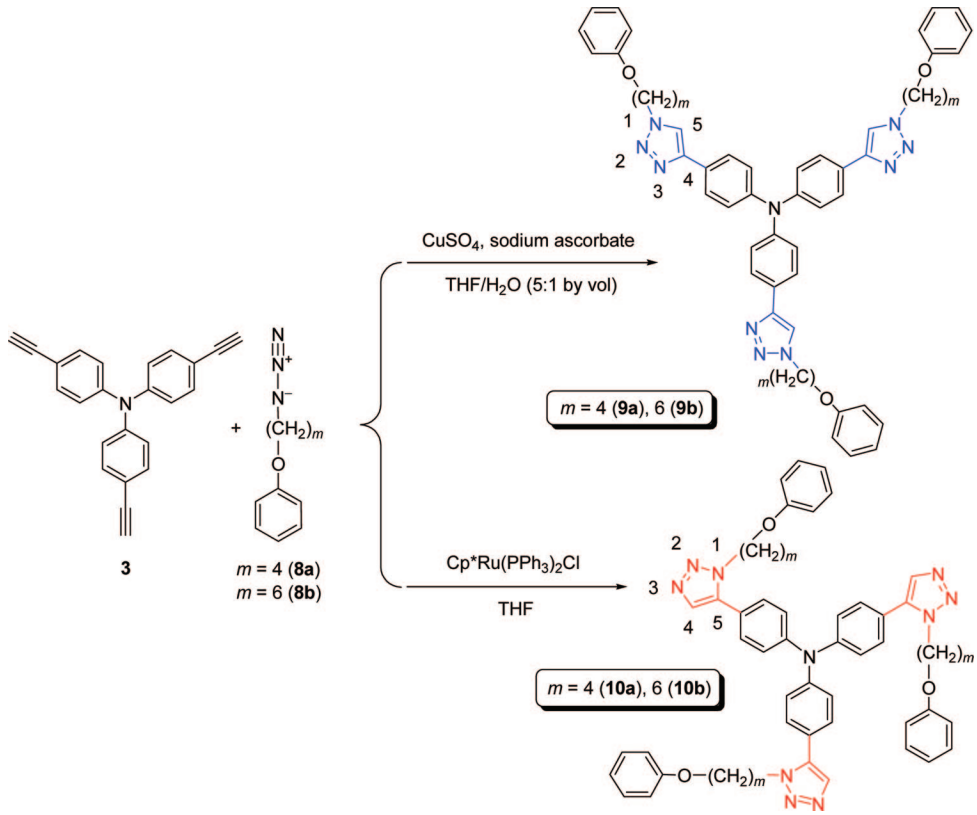

Scheme 5. Syntheses of Model Compounds of 1,4-Disubstituted 1,2,3-Triazoles 11 and 12

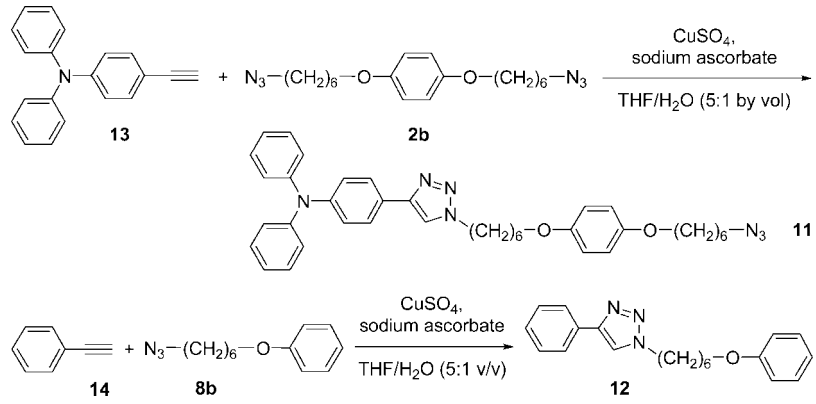

Triazole derivatives with **11** and without azido moieties **12** were designed and prepared as model compounds for the study of photolysis mechanisms of *hb*-PTAs. The reaction of an equimolar mixture of 4-ethynyl-*N,N*-diphenylbenzenamine (**13**) and 1,4-bis(6-azidohexyloxy)benzene (**2b**) afforded azidotriazole **11** in 28% yield, while the reaction of phenylacetylene (**14**) with 1-(6-azidohexyloxy)benzene (**8b**) produced 1-(6-phenoxyhexyl)-4-phenyl-1,2,3-triazole (**12**) in a yield as high as 88% (Scheme 5). Aminomonoyne **13** is more electron rich than phenylacetylene (**14**). The results of these model reactions once again confirm the electronic effect involved in the Cu(I)-catalyzed click reaction.

All the monomers and model compounds were characterized by spectroscopic methods, from which satisfactory analysis data were obtained [see Experimental Section and Supporting Information (Figures S1−S3) for details]. Unlike the AB_2 monomers used in the early studies,[11] the A_2 and B_3 monomers prepared in the present work are stable and can be stored in a dark place at room temperature for a long period of time. No structural changes caused by such undesired reactions as self-oligomerization were observed after the monomers had been kept in our laboratories for more than 6 months.

1,3-Dipolar Polycycloadditions of Diazides 2 and Triyne 3. In our previous study, we found that thermal polymerizations of diazides (N_3-R-N_3) and electron-deficient diynes (HC≡C−OCArCO−C≡CH) proceeded rapidly: heating 1,4-bis(6-azidohexyloxy)benzene and 3,3′-(1,6-hexylenedioxy)-bis(benzoylacetylene), for example, in a DMF/toluene mixture for a short period (e.g., 30 min) resulted in the formation of polymeric products. The polymerization conducted in an *N,N*-dimethylacetamide/toluene mixture at 100 °C for 6 h produced a linear PTA with an M_w value of 25 300 and an $F_{1,4}$ ratio of ∼92% in ∼96% yield.[13] The triyne **3** we prepared in this work is, however, electron-rich. Although it reacted with monoazides **8** in the presence of the Cu(I) and Ru(II) catalysts, it failed to undergo thermal cycloaddition after its mixture with **8a** was refluxed in dioxane for 24 h. It was thus intriguing to check

Table 1. Effect of Solvent on Thermal Polycycloaddition of Diazide 2a and Triyne 3[a]

no.	solvent	time (h)	yield (%)	$M_{w,r}$[b]	PDI[c]	$F_{1,4}$ (%)[d]
1	toluene	90	trace	1900	1.3	54
2	chlorobenzene	77	39.2	3900	1.7	52
3	*o*-dichlorofbenzene	77	50.1	5200	1.9	53
4	dioxane	72	79.7	5800	2.3	53

[a] Polymerization reactions carried out at 110 °C under nitrogen; $[\mathbf{3}]_0/[\mathbf{2a}]_0 = 2:3$; $[\mathbf{3}]_0 = 0.067$ M (for nos. 1 and 2), 0.1 M (for nos. 3 and 4). [b] Relative weight-average molecular weight estimated by gel permeation chromatography (GPC) in THF on the basis of a linear polystyrene calibration. [c] PDI = polydispersity index (M_w/M_n). [d] Molar fraction of 1,4-regioisomeric unit.

whether and how it would perform as a monomer in its thermal polymerizations with diazides **2**.

The attempted thermal polymerization of **3** with **2a** in toluene was virtually failed: after refluxing in the solvent for as long as ~4 days, only was a trace amount of hexane-insoluble product isolated (Table 1, no. 1). The regiostructure of the product was elucidated by NMR analysis (vide infra), from which an $F_{1,4}$ ratio of 54% was obtained. These data indicate that the thermal polymerization of the electron-rich triyne in the nonpolar solvent is very sluggish and practically regiorandom. The thermal polymerization, however, could be accelerated by enhancing the solvent polarity (Scheme 6). When the solvent was changed from less polar toluene to more polar dioxane, the polymerization time was shortened (from ~4 to 3 days) and the polymer yield was greatly increased (from ~0% to ~80%; cf. Table 1, nos. 1 and 4). The $F_{1,4}$ ratios of the polymers, however, remained unchanged within experimental error.

The thermal polymerizations of **3** with **2a** were further studied in an effort to optimize the process (Figure S4; Supporting Information). Under optimal conditions, **3** was polymerized with **2b**, affording an *hb*-*r*-P**1b** in ~76% yield (Table 2, no. 2). Its $M_{w,r}$ and PDI values were estimated by GPC to be 11 400 and 2.7, respectively. It should be noted that the GPC calibrated by linear polystyrene standards can significantly underestimate $M_{w,r}$ values of hyperbranched polymers.[16] Deffieux et al., for example, found that the relative molecular weights of their hyperbranched polystyrenes estimated by GPC were normally ~7-fold, sometimes even ~30-fold, lower than the absolute values determined by the laser light scattering (LLS) technique.[16b] We employed the LLS technique to measure the $M_{w,a}$ value of the polymer, which was found to be 177 500, about 14-fold higher than its $M_{w,r}$ value.

It became clear that triyne **3** could undergo thermal polymerization with diazides **2** in a polar solvent to produce high molecular weight polymers with regiorandom structure and macroscopic processability in good yields, albeit at a slow rate. To prepare regioregular polymers at a fast rate, we paid attention to the metal catalysts used in the azide−alkyne click reactions.[1,2] As the model reactions had proved that triyne **3** cyclized with monoazides **8** in the presence of the Cu(I) catalyst, we tried to use it to synthesize *hb*-PTAs through its polycycloaddition with diazides **2** (Scheme 7). Mixing **3**/**2a** with $CuSO_4$/sodium ascorbate under the standard click reaction conditions[1] caused instant formation of precipitates, which could not be dissolved in any common organic solvents (Table 2, no. 3). Similar results were obtained when **3** was subjected to the click polymerization with **2b**: mixing the monomer and catalyst solutions resulted in immediate gel formation. The "standard recipe" for the click reaction is thus not suitable for the synthesis of processable *hb*-PTAs, confirming the early observations by other research groups.[11]

The $CuSO_4$/sodium ascorbate catalyst was used in a THF/water mixture. The incompatibility between the growing *hb*-PTA species and the aqueous medium may have induced the polymers to aggregate and hence precipitate. To avoid the use of aqueous medium, we employed a nonaqueous click catalyst of $Cu(PPh_3)_3Br$[17] to initiate the click polymerization of triyne **3** with diazides **2**. The polymerization of **3** and **2a** conducted in the presence of $Cu(PPh_3)_3Br$ in DMF at 60 °C for 80 min produced an *hb*-1,4-P**1a** in ~46% (Table 2, no. 5), which was soluble in common organic solvents, including DCM, THF, DMF, and DMSO. Similarly, the polymerization of **3** and **2b** carried out in the nonaqueous medium afforded a soluble *hb*-1,4-P**1b** in ~52% yield. The Cu(I) catalysts have greatly accelerated the polycycloaddition process (e.g., 80 min at 60 °C), in comparison to the thermally activated system (e.g., 72 h at 101 °C).

The 1,5-regioselective click polymerization of **3** and **2** catalyzed by $Cp^*Ru(PPh_3)_2Cl$ proceeded even faster, in comparison to the Cu(I) system, thanks to the higher substrate tolerance of the Ru(II) complex. The Ru(II)-catalyzed polymerization of **3** and **2b** furnished a soluble *hb*-1,5-P**1b** in ~75% yield in as short as 30 min (Table 2, no. 7). The preparation of the Ru(II) complex, however, is a nontrivial job that requires high synthetic skills.[1e] Dichloro(pentamethylcyclopentadienyl)-ruthenium(III) oligomer $\{[Cp^*RuCl_2]_n\}$ is a precursor to $Cp^*Ru(PPh_3)_2Cl$ and can be facilely prepared in high yield by refluxing $RuCl_3 \cdot nH_2O$ and Cp*H in ethanol for a few hours.[18] Although we worried that the stable Ru(III) precursor may not work well as a click catalyst, it smoothly catalyzed the polycycloaddition of **3** and **2** at a moderate temperature (40 °C), producing soluble *hb*-1,5-P**1** polymers in high yields (>83%).

Processability, Stability, and Solubility. All the freshly prepared samples of *hb*-PTAs, including the regiorandom *hb*-*r*-P**1** and regioregular *hb*-1,4-P**1** and *hb*-1,5-P**1** polymers, are readily processable: thin solid films can be facilely prepared by static or spin casting of their 1,2-dichloroethane solutions onto solid substrates, such as silicon wafers, glass slides, and mica plates. All the polymers are thermally stable, irrespective of the polymerization processes by which they were prepared. As can be seen from the thermogravimetric analysis (TGA) curves shown in Figure S5 (Supporting Information), the *hb*-PTAs lose 10% of their original weights in the temperature region of 374−407 °C, indicative of a strong resistance to thermolysis. No glass transition temperatures were detected by the differential scanning calorimetry (DSC) measurements when the polymers were heated up to 200 °C.

The polymers prepared by the $Cu(PPh_3)_3Br$ catalyst (*hb*-1,4-P**1**), however, gradually became partially insoluble upon storage under ambient conditions. One possible reason for this solubility change is the postpolymerization reactions of the polymers catalyzed by the metallic residues trapped in the *hb*-1,4-P**1** samples. The copper species may have coordinated with the "old" amino functional groups in the monomer repeat units and/or the "new" triazole rings formed during the 1,3-dipolar polycycloaddition reactions.[19]

In a control experiment, we admixed a small amount of $CuSO_4$/sodium ascorbate with an *hb*-1,5-P**1** polymer prepared from the ruthenium-catalyzed click polymerization. The polymer became insoluble within a few minutes, although it remained soluble after storage for several months in the absence of the externally added copper catalyst. The copper species may have catalyzed the 1,3-dipolar cycloaddition reaction of the azido and ethynyl terminal groups on the peripheral surfaces of the polymer, making it cross-linked and hence insoluble. We tried to remove the catalyst residues by washing the *hb*-1,4-P**1** polymers with amine solvents, but the results were not satisfactory because of the poor solubility of the polymers in the hydrophilic solvents.

Another possible reason for the solubility change of *hb*-1,4-P**1** with storage is the aggregate formation in the solid state.

Scheme 6. Syntheses of *hb-r*-P1 Polymers by Thermal Polycycloadditions of Diazides 2 and Triyne 3

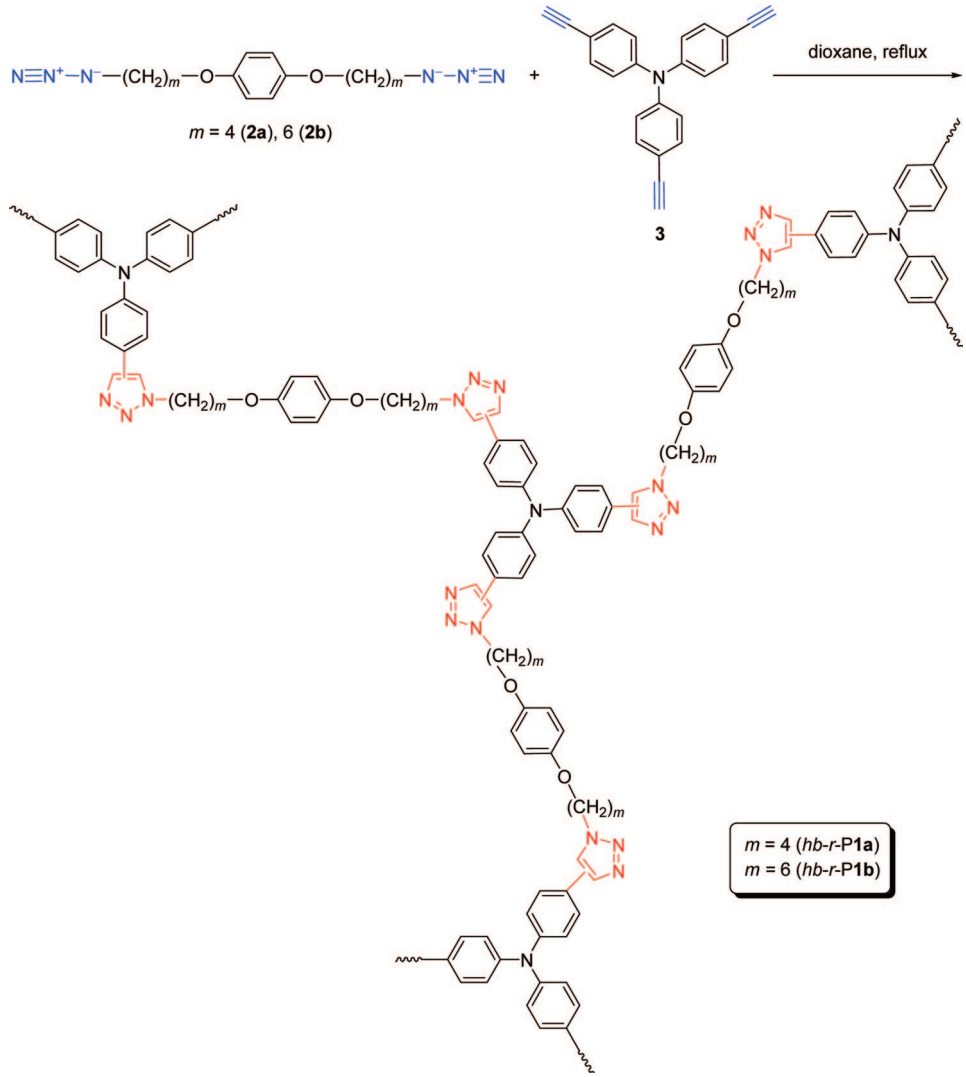

Table 2. Syntheses of Regiorandom and Regioregular *hb*-PTAs by Thermally Initiated and Metal-Catalyzed Polycycloadditions of Diazides 2 and Triyne 3[a]

no.	monomers	catalyst	solvent	temp (°C)	time (h)	polymer	yield (%)	$M_{w,r}$[b]	PDI[b]	$M_{w,a}$[c]
1	**2a** + **3**	(thermal)	dioxane	101	72.00	*hb-r*-P1a[d]	64.0	5500	2.0	
2	**2b** + **3**	(thermal)	dioxane	101	72.00	*hb-r*-P1b[e]	75.7	11400	2.7	177500
3	**2a** + **3**	$CuSO_4$/SA	THF/H_2O[f]	rt	inst.[g]	*hb*-1,4-P1a	gel[g]			
4	**2b** + **3**	$CuSO_4$/SA	THF/H_2O[f]	rt	inst.[g]	*hb*-1,4-P1b	gel[g]			
5	**2a** + **3**	$Cu(PPh_3)_3Br$	DMF	60	1.33	*hb*-1,4-P1a	46.3	2600	1.5	
6	**2b** + **3**	$Cu(PPh_3)_3Br$	DMF	60	1.33	*hb*-1,4-P1b	51.6	5000	2.0	
7	**2a** + **3**	$Cp^*Ru(PPh_3)_2Cl$	THF	60	0.33	*hb*-1,5-P1a	62.5[h]	5400	2.4	72800
8	**2b** + **3**	$Cp^*Ru(PPh_3)_2Cl$	THF	60	0.50	*hb*-1,5-P1b	74.9	9400	2.7	32200
9	**2a** + **3**	$[Cp^*RuCl_2]_n$	THF	40	2.00	*hb*-1,5-P1a	85.4	5000	1.8	
10	**2b** + **3**	$[Cp^*RuCl_2]_n$	THF	40	2.00	*hb*-1,5-P1b	83.2	7700	2.2	

[a] Polymerization reactions carried out under nitrogen; $[\mathbf{3}]_0/[\mathbf{2}]_0$ = 2:3, $[\mathbf{3}]_0$ = 0.12 M. Abbreviations: SA = sodium ascorbate; rt = room temperature. [b] Relative (r) value estimated in THF by GPC on the basis of a linear polystyrene calibration. [c] Absolute (a) value measured in THF (for no. 2) or DMF (for nos. 7 and 8) by the LLS technique. [d] $F_{1,4}$ = 53%. [e] $F_{1,4}$ = 50%. [f] Volume ratio: 5:1. [g] Instant gel formation (once the monomer and catalyst solutions were mixed). [h] Soluble fraction (total yield: 84.5%).

We "created" a simple molecule of tris[4-(1-methyl-1,2,3-triazol-4-yl)phenyl]amine (**15**) that resembles the cyclic unit of *hb*-1,4-P**1** and subjected it to theoretical stimulation, using AM1 Hamiltonian in the MOPAC package embedded in the Chem3D Ultra program. In the optimized conformation, the phenyl and triazole rings of the 1,4-isomer experience little steric interaction and can locate almost in the same plane (Chart 1A). During storage, the cyclic plates of the *hb*-1,4-P**1** polymers may gradually pack, with the aid of the $\pi-\pi$ stacking attractions between their aromatic units. This "physical cross-linking" process progressively knits more polymer molecules together and widens the three-dimensional networks, hence gradually decreasing the polymer solubility.

On the other hand, there exists steric repulsion between the phenyl and triazole rings in the 1,5-isomer **16**. The rings are therefore twisted out of coplanarity to alleviate the involved steric effect (Chart 1B). This twisted, nonplanar structure makes the cyclic units of *hb*-1,5-P**1** polymers difficult to pack in the solid state. The 1,5-regioregular polymers thus can maintain their good solubility for a long period of time. The *hb-r*-P**1** polymers

Scheme 7. Syntheses of Regioregular *hb*-PTAs by Transition-Metal-Catalyzed Click Polymerizations of Diazides 2 and Triyne 3

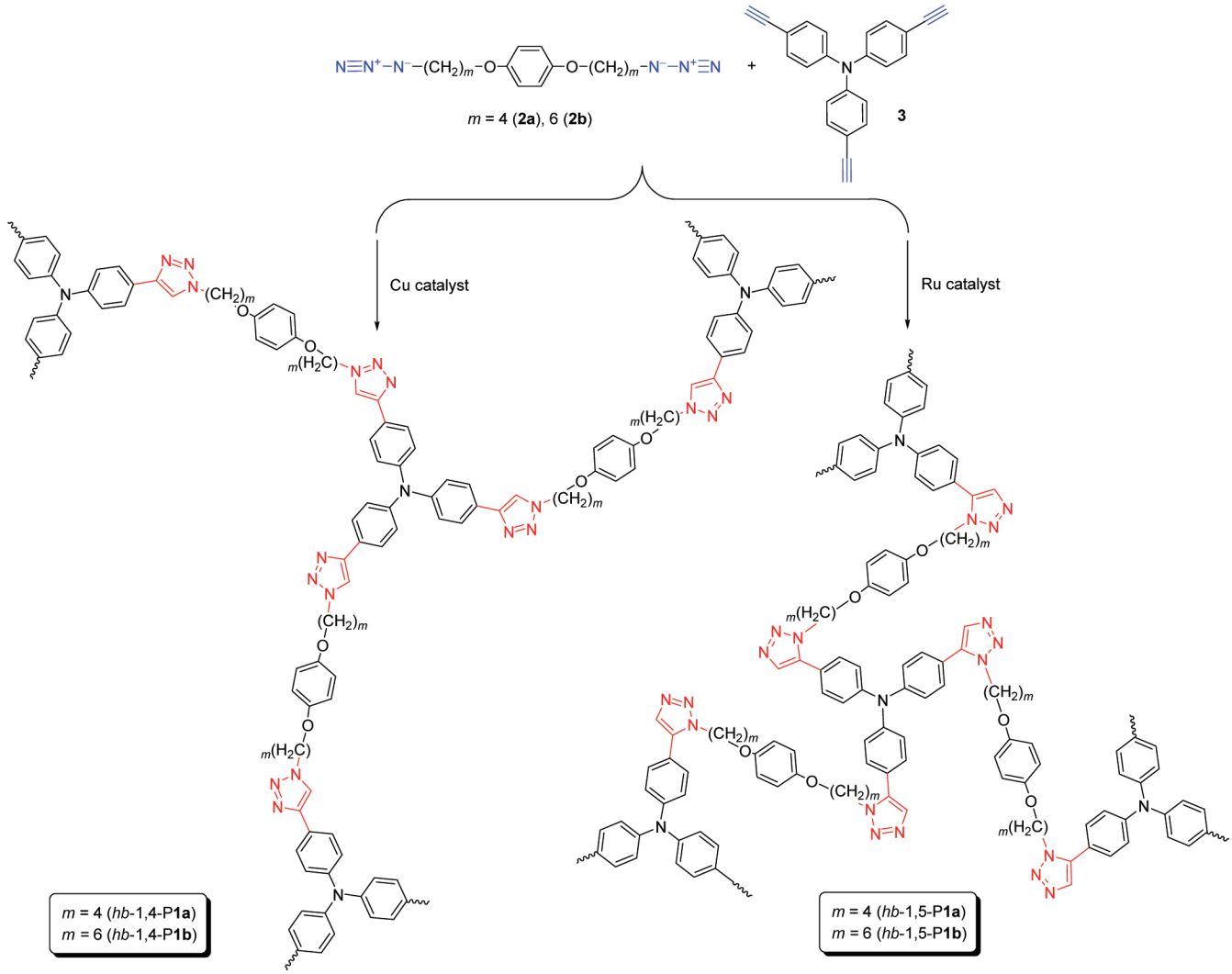

prepared by the thermal polymerizations possess a random regiostructure and would be difficult to pack in the solid state. In addition, no transition metal catalyst was used in the thermal polymerization process; in other words, no metallic residues were left in the polymers. The *hb-r*-P**1** polymers thus should have good solubility: indeed, the polymers remained soluble after they had been stored in the solid state under ambient conditions for several months.

Structural Characterization. The *hb*-PTA polymers were characterized spectroscopically, and all of the polymers gave analysis data corresponding to their expected molecular structures [see Experimental Section and Supporting Information (Figures S6−S9) for details]. Examples of the IR spectra of *hb-r*-P**1** polymers are shown in Figure 1; those of monomers **3** and **2a** are given in the figure for comparison. Monomer **3** absorbs at 3287 and 2104 cm^{-1} due to its ≡C−H and C≡C stretching vibrations, respectively. Monomer **2a** exhibits a strong absorption band at 2097 cm^{-1} associated with the stretching of its azido group. All these absorption bands become weaker in intensity in the spectrum of *hb-r*-P**1a** (Figure 1C). This suggests that while most of the ethynyl and azido groups of the monomers have been transformed to the triazole rings of the polymer by the polymerization reaction, some of the functional groups have not reacted, remaining in the polymer as parts of its linear (*L*) and terminal (*T*) units (cf. Chart 2).

The spectral profile of *hb-r*-P**1b** is similar to that of *hb-r*-P**1a** (cf. panels C and D of Figure 1), implying that the alkyl chain length exerts little effect on the polymer structure. The spectra of the regioregular polymers *hb*-1,4-P**1** (Figure S6) and *hb*-1,5-P**1** (Figure S7) are also similar (Supporting Information). These spectral data confirm that all the polymers share the same basic molecular structure comprising of multiple triazole rings. The IR spectral data, however, offer no information about the regioselectivity (1,4 or 1,5) of the polymerization reactions and the regioregularity ($F_{1,4}$ ratio) of the polymer products. We thus tried to use the NMR technique to tackle this important structural issue.

We first measured the ^{1}H NMR spectrum of *hb-r*-P**1b** in chloroform-*d*, the most commonly used deuterated solvent for NMR analysis. The spectrum of the polymer is shown in Figure 2, along with those of its monomers. The resonances of the ethynyl proton of triyne **3** and the methylene proton adjacent to the azido group of diazide **2b** occur at δ 3.06 and 3.28, respectively. Both peaks become weaker in the spectrum of the polymer. This substantiates the conclusion drawn from the IR analysis. Unfortunately, however, the protons of the phenyl and triazole rings all resonate in a narrow spectral range. The severe peak overlap makes it difficult to analyze the regiostructure of the polymer.

We then measured the ^{1}H NMR spectra of *hb-r*-P**1b** in other deuterated solvents and found that the spectrum taken in DMSO-d_6 was useful for regiostructural analysis. Figure 3 shows the NMR spectra of *hb-r*-P**1b** and its monomers (**3** and **2b**) as well as its model compounds (**9b** and **10b**) in DMSO-d_6. By

Chart 1. Simulated Conformations of (A) Tris[4-(1-methyl-1,2,3-triazol-4-yl)phenyl]amine (15) and (B) Tris[4-(1-methyl-1,2,3-triazol-5-yl)phenyl]amine (16)

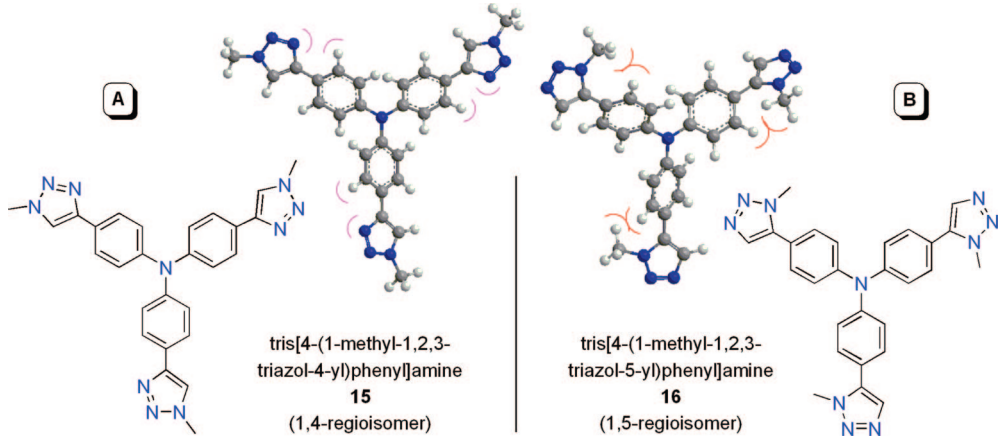

comparison with the spectra of the monomers and model compounds, the peaks of the polymer are readily assigned. Of great value is the peak at δ 8.60 arising from the resonance of the proton of the 1,4-isomeric unit (no. 47) of the polymer (Figure 3E). This peak is well separated from the peak at δ 7.89, which is associated with the resonances of the protons of the 1,5-isomeric unit of the polymer (no. 42) and the phenyl ring adjacent to its 1,4-isomeric unit (no. 46).

On the basis of above spectral analysis, the $F_{1,4}$ ratio of *hb-r*-P**1b** can be correlated with its NMR data as follows:

$$\frac{F_{1,4}}{F_{1,5}} = \frac{A_{47}}{A_{42,46} - 2A_{47}} \quad (1)$$

where $F_{1,5}$ is the fraction of its 1,5-isomeric unit, and A_{47} and $A_{42,46}$ are the integrated areas of peaks 47 and (42, 46), respectively. Because $F_{1,4} + F_{1,5} = 1$, eq 1 can be transformed to the following equation:

$$F_{1,4} = \frac{A_{47}}{A_{42,46} - A_{47}} \quad (2)$$

The $F_{1,4}$ ratio for *hb-r*-P**1b** was calculated to be 50% from eq 2 and the spectral data given in Figure 3. A similar equation was derived for calculating the regioregularity of *hb-r*-P**1a** [$F_{1,4} = A_{39}/(A_{34,38} - A_{39})$], from which its $F_{1,4}$ ratio was determined to be 53% (cf. Figure S2, Supporting Information).

The $F_{1,4}$ ratios of around 50% for the *hb-r*-P**1** polymers confirm that the thermal polymerizations of diazides **2** and

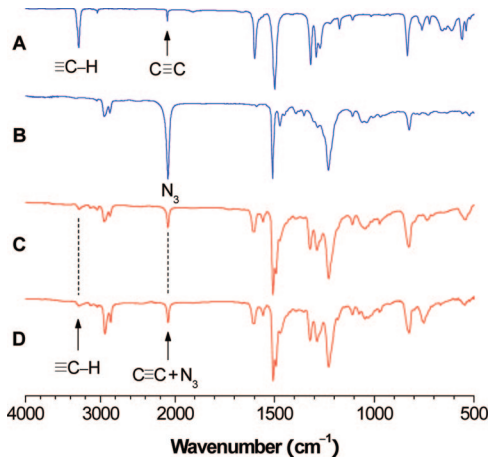

Figure 1. IR spectra of monomers **3**(A) and **2a** (B) and hyperbranched polymers *hb-r*-P**1a** (C) and *hb-r*-P**1b** (D).

electron-rich triyne **3** have proceeded in a regiorandom fashion. In our previous work, we found that the diazides and the electron-deficient diynes thermally polymerized regioselectively.[13] Evidently, the regioselectivity of the thermal polymerization is dramatically affected by the electronic structure of the alkyne monomer, offering a molecular engineering means for tuning the regioregularity of PTA.

It is well-known that the Cu(I)- and Ru(II)-catalyzed click reactions[1,2] yield 1,4- and 1,5-disubstituted 1,2,3-triazoles, respectively. As expected, the polymers obtained from the click polymerizations of **2b** and **3** initiated by the $Cu(PPh_3)_3Br$ and $Cp^*Ru(PPh_3)_2Cl$ catalysts exhibit strong and nil signals at δ 8.63, respectively (panels A and B of Figure 4). Different from $Cp^*Ru(PPh_3)_2Cl$ complex, $[Cp^*RuCl_2]_n$ oligomer possesses a Ru(III) center. The polymer prepared from this catalyst also gives a spectrum free of the diagnostic peak for the 1,4-isomeric unit at δ 8.63 (Figure 4C). This confirms that the 1,5-regioregular polymer can be prepared by the "simple", stable, and "cheap" Ru(III) complex. This also suggests the possibility that the Ru(III) center may have been in situ reduced to a Ru(II) active species during the click polymerization reaction. Similar results were obtained from the spectral analyses of the *hb*-1,4- and -1,5-P**1a** polymers prepared from the copper- and ruthenium-catalyzed click polymerizations of **2a** and **3** (Figure S8, Supporting Information).

Determination of Degree of Branching. An important structural parameter for a hyperbranched polymer is its degree of branching (DB), which is often determined by ^{1}H NMR spectral analysis.[10] It can been seen from Chart 2 that there exist six structural units in an *hb-r*-P**1**: one dendritic unit (*D*), two linear units [one with an unreacted ethynyl group (L_e) and another with an unreacted azido group (L_a)], and three terminal units [one with two ethynyl groups (T_{ee}), one with two azido groups (T_{aa}), and one with an ethynyl group and an azido group (T_{ea})]. We scrutinized with great care the NMR spectra of *hb-r*-P**1b** measured in different solvents, especially its peaks associated with the resonances of the triple bond and the azido group (actually its adjacent methylene unit), and found with delight that the spectrum taken in chloroform-*d* could be used for the calculation of DB value of the polymer.

To simplify the calculation, we assume that there are no side reactions such as loop formations in the azide−alkyne 1,3-dipolar polycycloaddition reactions. By comparing the NMR spectrum of *hb-r*-P**1b** with those of its monomers (**2b** and **3**; cf. Figure 2), it is found that the following relationships hold for the molar fractions of the six structural units (f_D, f_{Le}, f_{La}, f_{Tee}, f_{Taa}, and f_{Tea}):

Chart 2. Chemical Structures of Dendritic (*D*), Linear (*L*), and Terminal (*T*) Units of *hb-r*-P1 Polymers

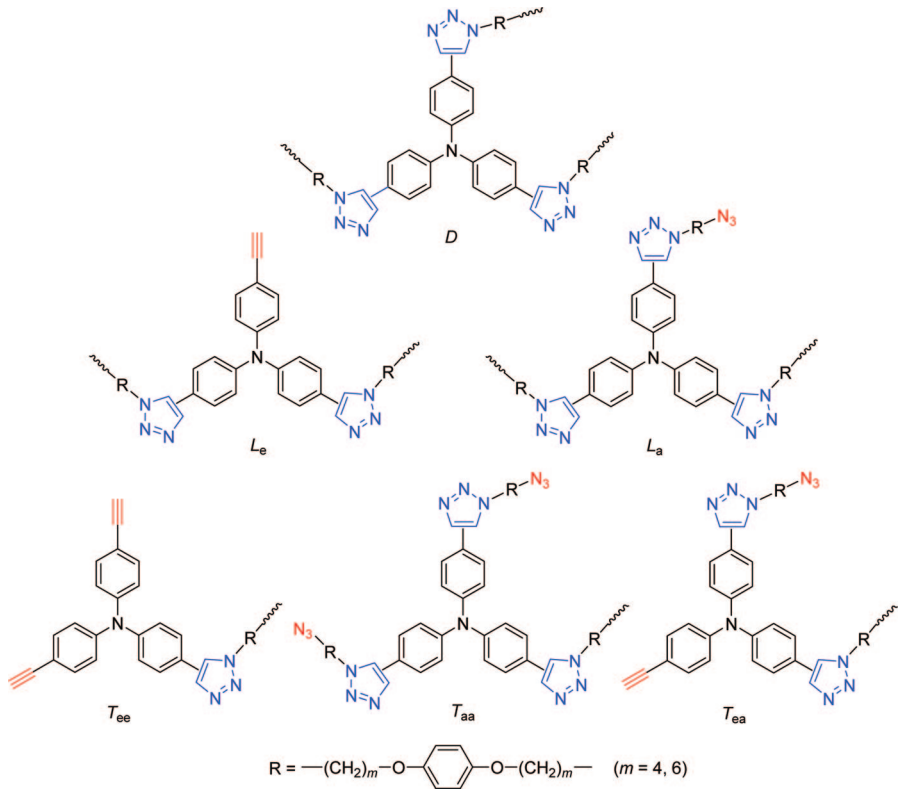

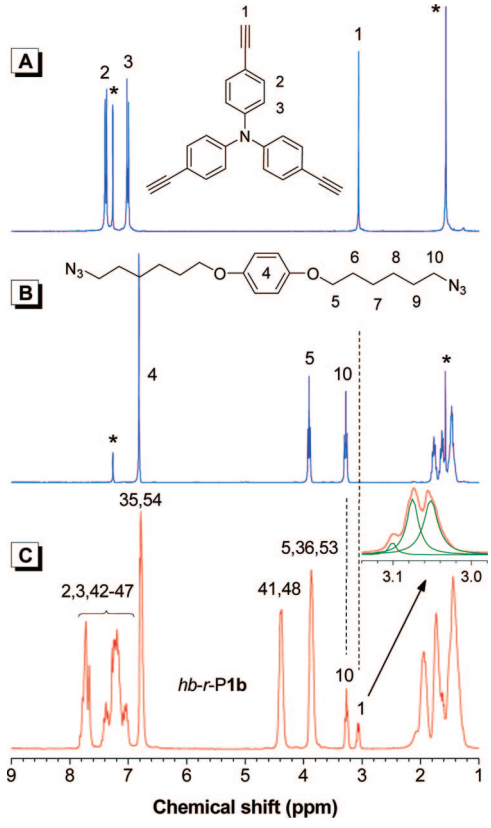

Figure 2. ^{1}H NMR spectra of chloroform-*d* solutions of monomers **3** (A) and **2b** (B) and their polymer *hb-r*-**P1b** (C) measured at room temperature. Labels of the resonance peaks of the polymer correspond to those given in Chart 3. The solvent and water peaks are marked with asterisks.

$$\frac{f_{Le}+2f_{Tee}+f_{Tea}}{2f_{La}+4f_{Taa}+2f_{Tea}}=\frac{A_1}{A_{10}} \tag{3}$$

$$\frac{f_{Le}+2f_{La}+2f_{Tee}+4f_{Taa}+3f_{Tea}}{3f_D+2f_{Le}+3f_L+f_{Tee}+3f_T+2f_{Tea}}=\frac{A_1+A_{10}}{A_{41,48}/2} \tag{4}$$

$$\frac{6f_D+4f_{Le}+8f_{La}+2f_{Tee}+10f_{Taa}+6f_{Tea}}{12f_D+12f_{Le}+12f_{La}+12f_{Tee}+12f_{Taa}+12f_{Tea}}=\frac{A_{35}}{A_{2,3,42-47}-A_{41,48}/2} \tag{5}$$

$$f_D+f_{Le}+f_{La}+f_{Tee}+f_{Taa}+f_{Tea}=1 \tag{6}$$

where A_1, A_{10}, $A_{41,48}$, $A_{35,54}$, and $A_{2,3,42-47}$ are the integrated areas of the resonance peaks 1, 10, (41, 48), (35, 54), and (2, 3, 42−47) as labeled in Figure 2 and Chart 3. From the integrated areas of the resonance peaks in the ^{1}H NMR spectrum, we get

$$\frac{A_1}{A_{10}}=\frac{0.077}{0.184} \tag{7}$$

$$\frac{A_1+A_{10}}{A_{41,48}/2}=\frac{0.077+0.184}{0.785/2} \tag{8}$$

$$\frac{A_{35,54}}{A_{2,3,42-47}-A_{41,48}/2}=\frac{1.018}{2.493-0.785/2} \tag{9}$$

From eqs 3–9, we can derive the following equation:

$$f_{Le}+2f_{Tee}+f_{Tea}=0.473 \tag{10}$$

Closer examination of the peak at δ 3.07 reveals that the peak contains three components, as shown in the inset of Figure 2C. Using a curve-fitting program and considering the electron-withdrawing effect of the triazole ring, we deconvoluted the resonance peak into three small peaks and assigned them from downfield to upfield to L_e, T_{ea}, and T_{ee}, with the ratio of their integrals calculated to be 0.14:1.00:1.21. Equations 11 and 12 are thus established:

Chart 3. Chemical Structure of *hb-r*-P1b with Labeling Scheme for Spectral Analysis

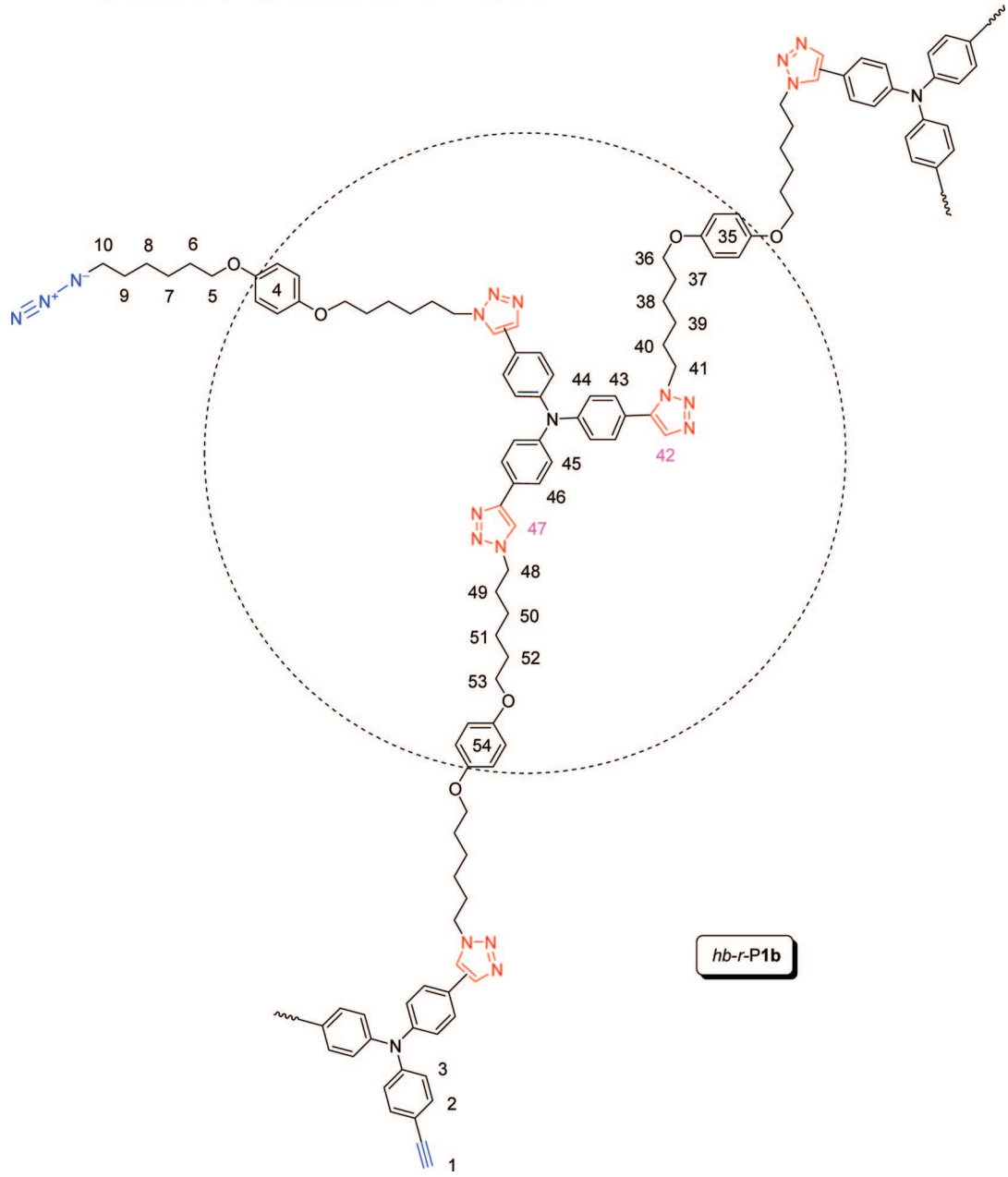

$$\frac{f_{Tee}}{f_{Le}} = \frac{1.21}{0.14} \tag{11}$$

$$\frac{f_{Tea}}{f_{Le}} = \frac{1.00}{0.14} \tag{12}$$

Further mathematical derivation gives f_{Le} as

$$f_{Le} = 0.02 \tag{13}$$

When this value is introduced into eq 3, we get eq 14:

$$f_{La} + 2f_{Taa} = 0.45 \tag{14}$$

For the *hb-r*-**P1b** polymer prepared from the 1,3-dipolar polycycloaddition reaction, it is reasonable to assume $f_{Taa} \geq 0$, from which we get $f_{La} \leq 0.45$.

DB of a hyperbranched polymer is defined as the ratio of the numbers of its dendritic and terminal units ($N_D + N_T$) versus the numbers of its total structural units ($N_D + N_T + N_L$).[20] According to this definition, DB of *hb-r*-**P1b** can be expressed as follows:

$$DB = \frac{f_D + f_{Tee} + f_{Taa} + f_{Tea}}{f_D + f_{Le} + f_{La} + f_{Tee} + f_{Taa} + f_{Tea}} \tag{15}$$

Incorporating eq 6 and $f_{La} \leq 0.45$ into eq 15 gives an estimated DB value of *hb-r*-**P1b**:

$$DB = 1 - f_{Le} - f_{La} \geq 1 - 0.02 - 0.45 \quad (DB \geq 0.53) \tag{16}$$

Because the azido functional groups are well separated by the flexible hexyl chains, the well-known and generally accepted "principle of equal reactivity of functional groups"[21] should be applicable to our system. Thus, according to Chart 2, eq 17 holds:

$$\frac{f_{Taa}}{f_{La}} = 2 \tag{17}$$

Combining eqs 17 and 14, we obtain

$$f_{La} = 0.09 \quad (18)$$

Eventually, under the assumptions we made above and within experimental errors, the DB value for *hb-r*-P**1b** is deduced to be

$$DB = 1 - f_{Le} - f_{La} = 1 - 0.02 - 0.09 = 0.89 \quad (19)$$

Taking the same approach, the DB value for *hb-r*-P**1a** is calculated to be 0.90, using eqs S1−S6 and NMR data (Figure S10) given in the Supporting Information. The similar DB values for *hb-r*-P**1a** (0.90) and *hb-r*-P**1b** (0.89) support the conclusion drawn from the spectroscopic analyses that the alkyl chain length exerts little effect on the polymer structure (vide supra). The high DB values duly verify the hyperbranched nature of the molecular structures of the polymers. The DB values of the *hb-r*-P**1** polymers are much higher than those of the "conventional" hyperbranched polymers (commonly ~0.50)[10,22] but close to those of some of the hyperbranched polyphenylenes we previously synthesized from the diyne polycyclotrimerizations (~0.79[23] and 0.78−1.00[24]). This is probably because the azide−alkyne polycycloaddition and the alkyne polycyclotrimerization share a similar growth mechanism of polymer species via aromatic ring formation.

Photophysical Properties. Linear PTAs have previously been prepared by other groups from Cu(I)-catalyzed polycycloadditions of conjugated arylenediazides and arylenediynes.[8] It was found that the absorption spectra of the polymers were "es-

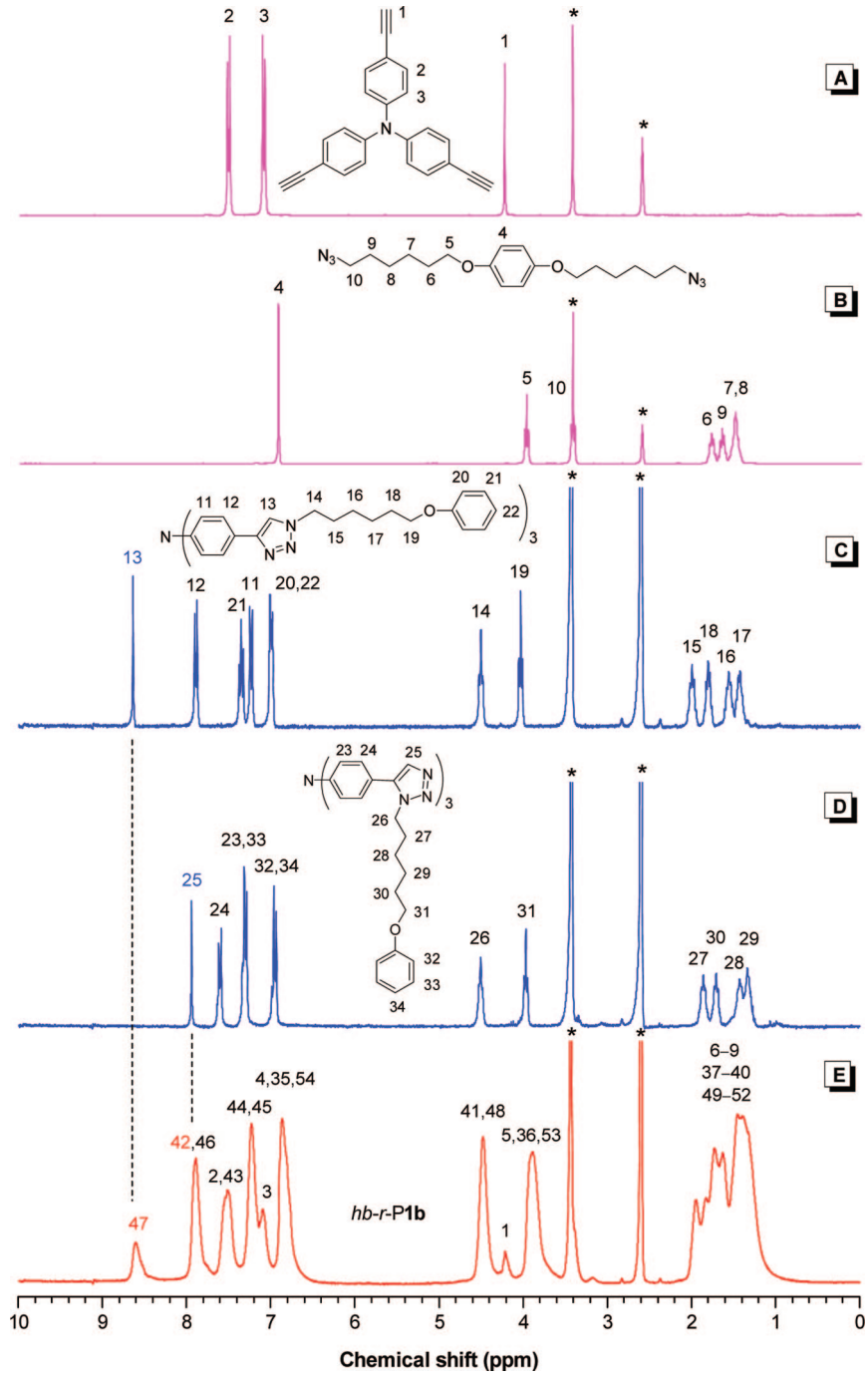

Figure 3. ^{1}H NMR spectra of DMSO-d_6 solutions of monomers **3** (A) and **2b** (B), model compounds **9b** (C) and **10b** (D), and polymer *hb-r*-P**1b** (E) measured at room temperature. Labels of the resonance peaks of *hb-r*-P**1b** correspond to those given in Chart 2. The solvent and water peaks are marked with asterisks.

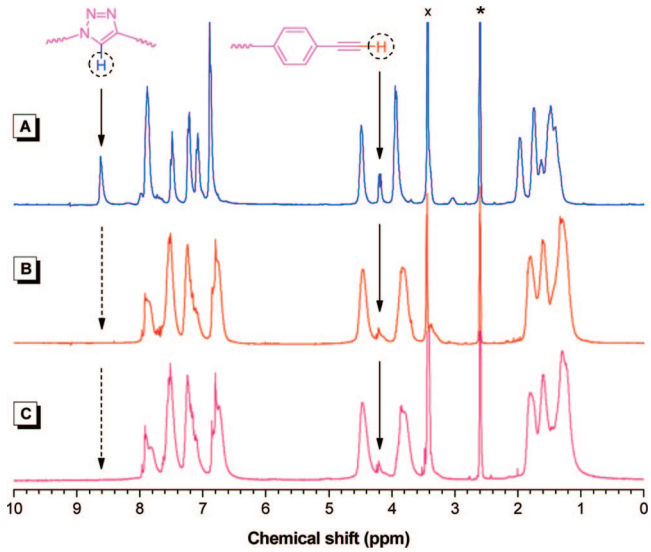

Figure 4. ^{1}H NMR spectra of (A) *hb*-1,4-P**1b** and (B, C) *hb*-1,5-P**1b** in DMSO-d_6 measured at room temperature. The peaks of water and solvent are marked with cross (×) and asterisk (*), respectively. The polymers were prepared by the click polymerizations of **2b** and **3** catalyzed by (A) $Cu(PPh_3)_3Br$, (B) $Cp^*Ru(PPh_3)_2Cl$, and (C) $[Cp^*RuCl_2]_n$.

sentially a superposition of those of the monomers used" with "no ground state interaction between the different moieties of the polymers" and that the polymers were "nonfluorescent in the solid state" although their dilute solutions emitted UV light with emission maxima (λ_{em}) of 355−379 nm.[8] This suggests that the solid-state luminescence has been efficiently quenched due to the $\pi-\pi$ stacking aggregation of the polymer chains.

The *hb*-PTAs synthesized in this work contain numerous conjugated triphenylamine and triazole units. Is there any electronic communication between these two aromatic moieties? How do the 1,4- and 1,5-regiostructures affect electronic conjugation and supramolecular aggregation? Are the polymers light-emitting, especially in the solid state? To answer these questions, we measured absorption and emission spectra of the *hb*-PTAs in dilute solutions and solid films. To gain insights into involved photophysical and aggregative processes, we also measured the spectra of some model compounds.

Model compounds of 1-(6-phenoxyhexyl)-4-phenyl-1,2,3-triazole (**12**) and triphenylamine absorb in the UV spectral region, with absorption maxima (λ_{ab}) at 251 and 305 nm, respectively (Figure 5A). The absorption spectrum of **10b**, a model compound with a 1,5-regiostructure, is peaked at 330 nm, which is 79 and 25 nm red-shifted from those of triazole **12** and triphenylamine, respectively. The spectrum of **9b**, a model compound with a 1,4-regiostructure, is further red-shifted from that of **10b**, indicative of a higher extent of electronic communication between triazole and triphenylamine units in the 1,4-isomer. This spectral data are in excellent agreement with the simulation results shown in Chart 1: the 1,4-isomer is conformationally more planar and hence electronically more conjugated.

The absorption spectra of *hb*-1,5- and -1,4-P**1b** polymers are also bathochromically shifted from those of triazole and triphenylamine compounds and are located in the vicinity of those of their corresponding model compounds with 1,5- (**10b**) and 1,4-regiostructures (**9b**; Figure 5B). This reveals that there exist ground-state interactions between the triphenylamine and triazole moieties in the polymers and that the electronic communications are dictated by the regioisomeric structures of triazolyl units. As expected, the absorption of *hb*-*r*-P**1b** occurs in the spectral region between those of its regioregular counterparts of *hb*-1,5-P**1b** and *hb*-1,4-P**1b** because the regiorandom polymers contains ∼50% of the 1,5- and 1,4-regioisomeric units. Also as anticipated, similar spectral data were obtained in the *hb*-P**1a** series (Figure S11, Supporting Information) because the length of alkyl chain does not affect the electronic communication between the aromatic moieties in the polymers.

The absorption spectrum of the thin film of model compound **9b** is bathochromically shifted from that of its dilute solution (Figure 6A), suggestive of aggregate formation of its aromatic moieties through $\pi-\pi$ stacking interaction in the solid state. The solution of **9b** exhibits a symmetrically shaped emission spectrum with a λ_{em} of 399 nm, whereas its film displays a broad, red-shifted spectrum extending into long wavelength region (up to ∼650 nm), characteristic of the emission of aggregative species, such as dimers or excimers. Its regioisomeric counterpart with a 1,5-linkage, viz. **10b**, gives similar spectral data: both absorption and emission spectra of the film are bathochromically shifted from those of the solution. Although weaker in intensity in comparison to its dimer emission at 450 nm, the monomer emission of the film of **10b** is still discernible at ∼400 nm as a shoulder peak. Moreover, the emission spectrum of **10b** is narrower than that of **9b** as a whole, with the full width at half-maximum (fwhm) of the former (61 nm) being only about half of the latter (114 nm). These spectral data suggest that the aggregation in **10b** is not as severe as in **9b**, probably because the more twisted conformation of the former has impeded the aggregate formation.

The solutions of the *hb*-PTAs emitted deep blue light of 409−416 nm, with fluorescence quantum yields of 14−43% (Figure 6 and Table 3). The emission spectra of their films are red-shifted from those of their solutions and are even broader than those of the films of their corresponding model compounds. As can be seen from Figure 6, the spectrum of the film of *hb*-1,4-P**1b** is broader than that of its model compound **9b**. The film spectrum covers almost the entire visible spectral region, with an fwhm of 133 nm, which is more than 2-fold wider than that of its solution (64 nm; Table 3, no. 2). The "monomer" emission of *hb*-1,5-P**1b** film becomes weaker, in comparison to its "dimer" or excimer emission (Figure 6E). The *hb*-*r*-P**1b** film also shows a broad emission spectrum. Similar spectral data are obtained in the series of *hb*-P**1a** polymers (Table 3 and Figure S12, Supporting Information). These results indicate that the aromatic moieties in the *hb*-PTAs are aggregated in the solid state.

The extents of chromophore aggregation in the *hb*-PTAs, however, are not as severe as in the linear PTA system, in which the solid films became totally nonfluorescent.[8] The aromatic units strung in the linear PTA chains were such planar plates as phenyl, pyridyl, fluorenyl, and triazolyl groups, which can be stacked or piled up via $\pi-\pi$ interaction in the solid state. The triphenylamino units embedded in the *hb*-PTAs are nonplanar and hence not easy to pack well. Different from the linear PTA chains, the *hb*-PTA spheres are also difficult to align well. These are probably the reasons why the aggregation is less developed in the *hb*-PTAs and why the polymers are still luminescent in the solid state.

Fluorescent Photopatterning. Since the films of the *hb*-PTAs are emissive, we tried to utilize them to create fluorescent images. Luminescent polymers with good film-forming ability and high photolysis efficiency are promising candidate materials to be used in the photoresist processes for the generation of fluorescent patterns,[25] which have potential applications in liquid crystal displays, light-emitting diodes, medicinal diagnostic biochips, etc.[26,27] The *hb*-PTAs are soluble and film-forming. They contain many azido, ethynyl, and triazolyl functional

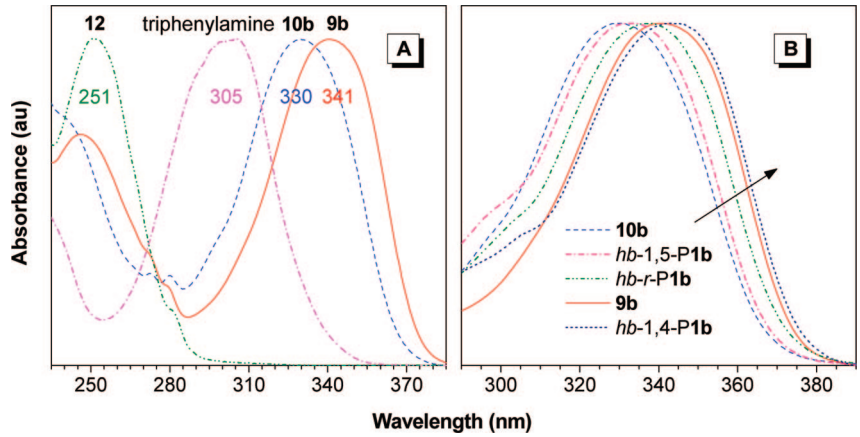

Figure 5. Normalized absorption spectra of DCM solutions of (A) model compounds **9b**, **10b**, 1-(6-phenoxyhexyl)-4-phenyl-1,2,3-triazole (**12**), and triphenylamine and (B) regioregular and regiorandom *hb*-PTAs and model compounds **9b** and **10b**. Solution concentration: (A) ~1 μM; (B) ~1.5 μg/mL (for polymer), ~1 μM (for model compound).

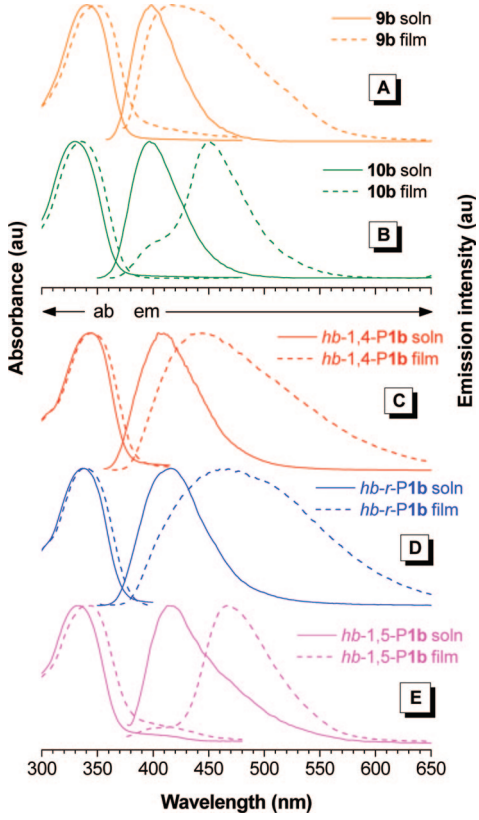

Figure 6. Normalized absorption (ab) and emission (em) spectra of DCM solutions (~1.5 μg/mL) and solid films of model compounds **9b** and **10b** and *hb*-PTAs. Excitation wavelength (nm): (A) **9b**: 341 (soln), 351 (film); (B) **10b**: 330 (soln), 335 (film); (C) *hb*-1,4-P**1b**: 343 (soln), 344 (film); (D) *hb-r*-P**1b**: 337 (soln), 340 (film); (E) *hb*-1,5-P**1b**: 336 (soln), 346 (film).

groups, which may be photolyzed, thus making the polymers photosusceptible.

When a thin film of *hb-r*-P**1a** was irradiated with a UV light (365 nm) for 5 min through a copper negative photomask, the exposed region of the film was rendered cross-linked and hence insoluble. After the film was developed with 1,2-dichloroethane, a three-dimensional negative photoresist pattern was generated (Figure 7A). The high quality of the pattern (sharp line edges, uniform film thickness, etc.) is clearly seen under the normal laboratory lighting, although the photoresist process has not yet been optimized. The pattern is fluorescent: the patterned lines emit white light upon shining with a UV lamp (Figure 7B).

Table 3. Photophysical Properties of DCM Solutions and Solid Films of *hb*-PTAs[a]

		λ_{ab} (nm)		λ_{em} (nm)				
no.	polymer	solution	film	solution	fwhm	Film	fwhm	Φ_F (%)
1	*hb*-1,4-P**1a**	345	344	409	63	442	120	21
2	*hb*-1,4-P**1b**	343	344	409	64	449	133	14
3	*hb-r*-P**1a**	338	339	415	67	449	127	38
4	*hb-r*-P**1b**	338	340	416	67	462	155	43
5	*hb*-1,5-P**1a**	336	341	416	77	466	68	32
6	*hb*-1,5-P**1b**	334	346	414	69	467	72	28

[a] Abbreviations: λ_{ab} = absorption maximum, λ_{em} = emission maximum, fwhm = full width at half-maximum, and Φ_F = fluorescence quantum yield, measured in DCM using 9,10-diphenylanthracene in cyclohexane (Φ_F = 90%) as standard.

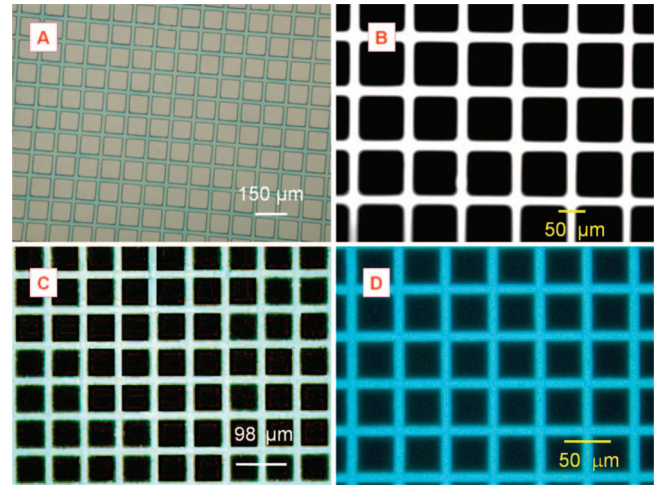

Figure 7. Photoresist patterns generated by photo-cross-linking of (A, B) *hb-r*-P**1a**, (C) *hb*-1,4-P**1a**, and (D) *hb*-1,5-P**1a** for 5 min in air; photographs taken under (A) normal laboratory lighting and (B−D) UV illumination.

Fluorescent patterns can also be generated by the UV photolyses of the regioregular *hb*-PTAs. The colors of the emissions from their photopatterns are, however, different. The light emitted from the pattern generated from the photolysis of *hb*-1,4-P**1a** is yellow in color, whereas that from *hb*-1,5-P**1a** is blue when observed by naked eyes (although the emission colors shown in panels C and D of Figure 7 are somewhat distorted by the photographing process[28]). The emission color of *hb*-1,4-P**1a** is redder than that of *hb*-1,5-P**1a**, which is understandable, because the former is more electronically conjugated and morphologically aggregated than the latter. This also explains

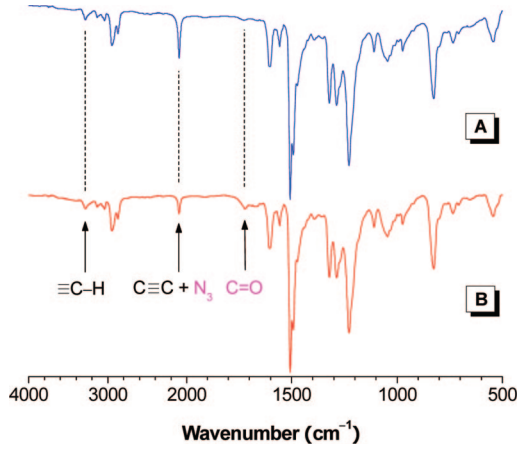

Figure 8. IR spectra of *hb-r*-P**1a** (A) before and (B) after UV irradiation for 5 min.

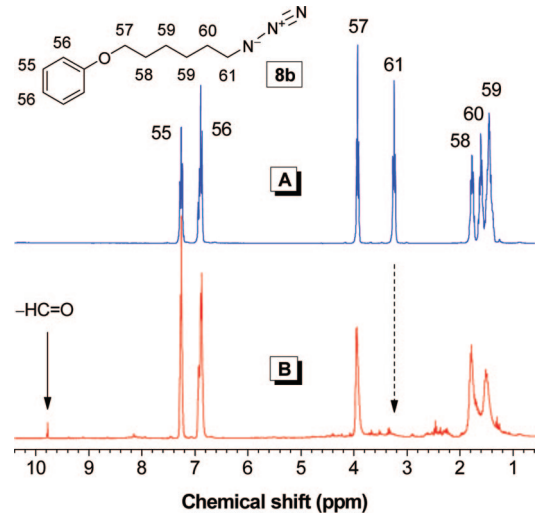

Figure 9. ^{1}H NMR spectra of $CDCl_3$ solutions of **8b** (A) before and (B) after UV irradiation for 10 h.

why *hb-r*-P**1a** emits a white light: the regiorandom polymer contains a roughly equal amount of 1,4- and 1,5-isomeric units, and the mixing of the complementary yellow and blue colors of the light emitted from the two units results in the light emission of a white color.[29] Similarly, the photopatterns generated from the films of *hb*-1,4-P**1b**, *hb*-1,5-P**1b**, and *hb-r*-P**1b** emit yellow, blue, and white light, respectively, demonstrating that the emission colors of the *hb*-PTA films are hardly affected the lengths of their alkyl chains.

The exposure of the *hb-r*-P**1a** film to the UV irradiation results in a decrease in the intensity of its IR absorption band at 2098 cm^{-1} (Figure 8). This band is assignable to the stretching vibrations of the ethynyl (C≡C) and azido (N_3) groups, but the decrease in the band intensity is probably mainly due to the photolysis of the azido group because the intensity of the ≡C−H band at 3283 cm^{-1} maintains almost unchanged. On the other hand, a new band associated with carbonyl (C═O) stretching appears at 1720 cm^{-1}, indicating that the polymer is oxidized during the photolysis process. The studies of the structural changes of the polymers accompanying the photolysis processes by the wet spectroscopic methods such as NMR are hampered by the insolubility of the photo-cross-linking products.

We thus conducted the photolysis reactions of some small model compounds, in the hope that their photolysis products can be caught by NMR spectroscopy. Model compound **11** contains triazolyl and azido groups but no ethynyl group. Its UV photolysis leads to the formation of an insoluble product, excluding the possibility that the ethynyl group is involved in the photolysis process of the azidotriazole compound. Model compound **12** contains a triazolyl group but no azido group. It remains soluble, and its NMR spectrum remains unchanged even after it has been irradiated by a UV lamp for 12 h, implying that the triazolyl group has not participated in the photo-cross-linking process.

Since the two model reactions discussed above have excluded the possible involvement of the ethynyl and triazolyl groups, the azido group must have been responsible for the photo-cross-linking reaction. This conclusion is further substantiated by another model reaction, in which a compound containing an azido group (**8b**) is irradiated by a UV lamp. The resonance peak of the protons of the methylene group adjacent to the azido group at δ 3.24 (no. 61) disappears after the photoirradiation due to the photolysis of the azido group (Figure 9). A new peak assignable to the resonance of an aldehyde proton appears at δ 9.78, indicating that the model compound is oxidized during its photolysis process.

The above experimental results suggest that the photo-cross-linking process of the *hb*-PTA starts from the photolysis of its azido group (Scheme 8). UV irradiation of *hb*-P**1** cleaves the $N^-{-}N^+$ bond of the azido group, releases a molecule of nitrogen, and generates an active nitrene radical (**17**).[30] Combination of the nitrene radical in **17** with that in another denitrogenated polymer results in the formation of **18**, a cross-linking product. The azo group hooking up two *hb*-PTA polymers can be broken by photoinduced homolysis, releasing another nitrogen molecule and yielding another polymer radical (**19**).[30] Coupling of two radicals furnishes anther cross-linking product **20**. Since the polymer contains numerous azido groups as verified by the spectral analysis and mathematical derivatization, the reaction routes of **17** → **18** and **19** → **20** will repeat, eventually leading to the formation of heavily cross-linked products that are insoluble in any organic solvents. The radical in **19** can also react with oxygen, thus transforming the methylene group adjacent to the azido group to an aldehyde species (**21**).

Concluding Remarks

In this work, we established an effective $A_2 + B_3$ route to soluble *hb*-PTAs. The diazide **2** and triyne **3** monomers were easy to prepare and free of the self-oligomerization problem encountered in the AB_2 system.[11] The thermally activated and metal-catalyzed polycycloadditions afforded regiorandom and regioregular *hb*-PTAs with high molecular weights (M_w up to $\sim 180 \times 10^3$). The solubility problem of *hb*-1,4-P**1** was solved by using nonaqueous catalyst of $Cu(PPh_3)_3Br$ to initiate the click polymerizations in DMF. $Cp^*Ru(PPh_3)_2Cl$ and its inexpensive, stable precursor $[Cp^*RuCl_2]_n$ were found to exhibit high catalytic activity to the electron-rich triyne monomer and smoothly catalyzed the click polymerizations in a regioselective manner, furnishing *hb*-1,5-P**1** in high yields (>83%). The *hb*-1,4-P**1** and *hb*-1,5-P**1** polymers are soluble and film-forming, representing the first examples of regioregular *hb*-PTAs with macroscopic processability.

The good solubility of the polymers enabled us to elucidate their structures spectroscopically. Using model compounds, we determined the regiostructures (1,4- and 1,5-linkages) and regioregularities ($F_{1,4}$ ratios) of the *hb*-PTAs. Through mathematic derivatization, the BD values of *hb-r*-P**1** were calculated to be ~90%. The *hb*-1,5-P**1** polymers were found to exhibit better solubility, shorter conjugation, bluer luminescence, and milder aggregation compared to their *hb*-1,4-P**1** counterparts. This was rationalized on the basis of regiostructural and steric effects: the aromatic units in the former are conformationally

Scheme 8. Proposed Photo-Cross-Linking Mechanism for *hb*-PTA

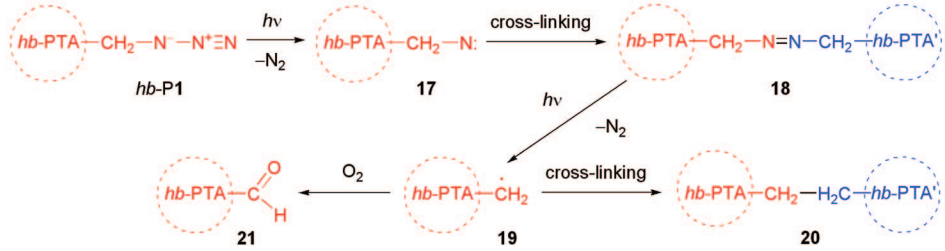

more twisted than the latter. We succeeded in generating fluorescent images with blue, yellow, and white emissions by irradiating *hb*-1,4-P**1**, *hb*-1,5-P**1**, and *hb*-*r*-P**1** films, respectively, demonstrating that photopatterns with different emission colors can be achieved by photolyses of the polymers with same chemical formulas but different regiostructures. This offers an attractive way to tune the emission color of a polymer film: simply changing the regiostructure of the same polymer without going through the trouble of synthesizing a new polymer with a different chemical structure.

Experimental Section

General information about materials and instrumentations, experimental procedures for the syntheses of the monomers and the model compounds, and structural characterization data for the monomers and the model compounds are given in the Supporting Information.

All the polymerization reactions and manipulations were carried our under nitrogen using Schlenk techniques in a vacuum line system or an inert atmosphere glovebox, except for the purifications of the polymers, which were conducted in an open atmosphere. Numerical spectral data for all the polymers, including *hb*-*r*-P**1**, *hb*-1,4-P**1**, and *hb*-1,5-P**1**, are given in the Supporting Information.

Thermally Activated Regiorandom 1,3-Dipolar Polycycloaddition (Scheme 6). Into a 20 mL Schlenk tube with a stopcock in the side arm were added **2** (0.6 mmol) and **3** (0.4 mmol). The tube was evacuated and refilled with nitrogen three times through the side arm. Freshly distilled dioxane (3.5 mL) was then injected into the tube to dissolve the monomers. The reaction mixture was refluxed for 72 h. After cooling to room temperature, the solution was diluted with a small amount of chloroform and then added dropwise to 300 mL of a hexane/chloroform mixture (10:1 by volume) through a cotton filter under stirring. The precipitate was allowed to stand overnight and was then collected and dried to a constant weight in a vacuum oven at room temperature.

Copper-Catalyzed 1,4-Regioregular Click Polymerization (Scheme 7). Into a 20 mL Schlenk tube with a stopcock in the side arm were added **2** (0.3 mmol), **3** (0.2 mmol), and $Cu(PPh_3)_3Br$ (0.012 mmol) under nitrogen in a glovebox. Dry DMF (1.7 mL) was injected into the tube to dissolve the monomers and catalyst. The reaction mixture was stirred at 60 °C for 80 min. Afterward, the mixture was diluted with chloroform and then added dropwise to 100 mL of a hexane/chloroform mixture (10:1 by volume) via a cotton filter under stirring. The precipitate was allowed to stand overnight and was then collected and dried to a constant weight in a vacuum oven at room temperature.

Ruthenium-Catalyzed 1,5-Regioregular Click Polymerization (Scheme 7). Into a 20 mL Schlenk tube with a stopcock in the side arm were added **2** (0.45 mmol), **3** (0.3 mmol), and $Cp^*Ru(PPh_3)_2Cl$ (0.018 mmol) under nitrogen in a glovebox. Freshly distilled THF (2.5 mL) was then injected into the tube to dissolve the monomers and catalyst. The reaction mixture was heated at 60 °C for 20 or 30 min. The mixture was then diluted with a small amount of THF and added dropwise to 300 mL of a mixture of hexane/chloroform (10:1 by volume) through a cotton filter under stirring. The precipitate was allowed to stand overnight and was then collected and dried to a constant weight in a vacuum oven at room temperature. Similarly, the polymerizations of **2** (0.15 mmol) and **3** (0.1 mmol) were carried out in the presence of $[Cp^*RuCl_2]_n$ (6.7 μmol) at 40 °C for 2 h.

Generation of Fluorescent Images via Polymer Photolyses. Photo-cross-linking reactions of the polymer films were initiated by the irradiation of a 365 nm UV light with an intensity of ~30 mW/cm^2. The films were prepared by spin-coating the polymer solutions (~2 wt % in 1,2-dichloroethane) at 800 rpm for 9 s and then at 2000 rpm for 60 s on precleaned silicon wafers. The films were dried in a vacuum oven at room temperature overnight. The photoresist patterns were prepared on the silicon wafers using copper negative photomasks. After UV irradiation, the films were developed in 1,2-dichloroethane for 40 s and then dried at room temperature overnight under reduced pressure. Fluorescent images of the patterns were taken on an Olympus BX41 fluorescent optical microscope with a 330−385 nm wide band UV excitation.

Acknowledgment. This work was partly supported by the Research Grants Council of Hong Kong (602707, 602706 and HKU2/05C), the National Natural Science Foundation of China (20634020), and the Ministry of Science & Technology of China (2002CB613401). B.Z.T. thanks the support from the Cao Guangbiao Foundation of Zhejiang University.

Supporting Information Available: Text describing general information about the materials and instrumentations and providing the experimental procedures and analysis data for the monomers, model compounds, and polymers; IR spectra of model compounds **9** and **10** and polymers *hb*-1,4-P**1** and *hb*-1,5-P**1**; ^{1}H NMR spectra of monomers **3** and **2a**, model compounds **9a** and **10a**, and polymers *hb*-*r*-P**1a**, *hb*-1,4-P**1a**, and *hb*-1,5-P**1a**; ^{13}C NMR spectra of model compounds **9** and **10** and polymers *hb*-*r*-P**1**, *hb*-1,4-P**1**, and *hb*-1,5-P**1**; chemical structure of *hb*-*r*-P**1a** with labeling scheme for spectral analysis; figure showing the effect of concentration of triyne **3** on its thermally activated polycycloaddition with diazide **2a** in dioxane; TGA thermograms of *hb*-P**1** polymers; and absorption and emission spectra of the solutions and films of the model compounds and polymers. This material is available free of charge via the Internet at http://pubs.acs.org.

References and Notes

(1) (a) Tornøe, C. W.; Meldal, M. In *Peptides: the Wave of the Future*; Lebel, M., Houghten, R., Eds.; American Peptide Society: San Diego, 2001; pp 263−264. (b) Kolb, H. C.; Finn, M. G.; Sharpless, K. B. *Angew. Chem., Int. Ed.* **2001**, *40*, 2004. (c) Rostovtsev, V. V.; Green, L. G.; Fokin, V. V.; Sharpless, K. B. *Angew. Chem., Int. Ed.* **2002**, *41*, 2596. (d) Tornøe, C. W.; Christensen, C.; Meldal, M. *J. Org. Chem.* **2002**, *67*, 3057. (e) Zhang, L.; Chen, X.; Xue, P.; Sun, H. H. Y.; Williams, I. D.; Sharpless, K. B.; Fokin, V. V.; Jia, G. *J. Am. Chem. Soc.* **2005**, *127*, 15998. (f) Majireck, M. M.; Weinreb, S. M. *J. Org. Chem.* **2006**, *71*, 8680.

(2) For selected examples of reviews, see: (a) Wang, Q.; Chittaboina, S.; Barnhill, H. N. *Lett. Org. Chem.* **2005**, *2*, 136. (b) O'Reilly, R. K.; Joralemon, M. J.; Wooley, K. L.; Hawker, C. J. *Chem. Mater.* **2005**, *17*, 5976. (c) Bock, V. D.; Hiemstra, H.; van Maarseveen, J. H. *Eur. J. Org. Chem.* **2006**, 51. (d) Boldt, G. E.; Dickerson, T. J.; Janda, K. D. *Drug Discovery Today* **2006**, *11*, 143. (e) Sohma, Y.; Kiso, Y. *Chem. Biol. Chem* **2006**, *7*, 1549. (f) Braunschweig, A. B.; Dichtel,

W. R.; Miljanic, O. S.; Olson, M. A.; Spruell, J. M.; Khan, S. I.; Heath, J. R.; Stoddart, J. F. *Chem. Asian J.* **2007**, *2*, 634. (g) Diez-Gonzalez, S.; Nolan, S. P. *Synlett* **2007**, 2158. (h) Aprahamian, I.; Miljanic, O. S.; Dichtel, W. R.; Isoda, K.; Yasuda, T.; Kato, T.; Stoddart, J. F. *Bull. Chem. Soc. Jpn.* **2007**, *80*, 1856. (i) Devaraj, N. K.; Collman, J. P. *QSAR Comb. Sci.* **2007**, *26*, 1253. (j) Salisbury, C. M.; Cravatt, B. F. *QSAR Comb. Sci.* **2007**, *26*, 1229. (k) Pieters, R. J.; Rijkers, D. T. S.; Liskamp, R. M. J. *QSAR Comb. Sci.* **2007**, *26*, 1181.

(3) Huisgen, R. In *1,3-Dipolar Cycloaddition Chemistry*; Padwa, A., Ed.; Wiley: New York, 1984; pp 1−176.

(4) For reviews, see: (a) Angell, Y. L.; Burgess, K. *Chem. Soc. Rev.* **2007**, *36*, 1674. (b) Moses, J. E.; Moorhouse, A. D. *Chem. Soc. Rev.* **2007**, *36*, 1249. (c) Dondoni, A. *Chem. Asian J.* **2007**, *2*, 700. (d) Nandivada, H.; Jiang, X. W.; Lahann, J. *Adv. Mater.* **2007**, *19*, 2197. (e) Wu, P.; Fokin, V. V. *Aldrichimica Acta* **2007**, *40*, 7. (f) Molteni, G. *Heterocycles* **2006**, *68*, 2177. (g) Binder, W. H.; Kluger, C. *Curr. Org. Chem.* **2006**, *10*, 1791. (h) Kolb, H. C.; Sharpless, K. B. *Drug Discovery Today* **2003**, *8*, 1128.

(5) For reviews, see: (a) Fournier, D.; Hoogenboom, R.; Schubert, U. S. *Chem. Soc. Rev.* **2007**, *36*, 1369. (b) Lutz, J. F. *Angew. Chem., Int. Ed.* **2007**, *46*, 1018. (c) Voit, B. *New J. Chem.* **2007**, *31*, 1139. (d) Binder, W. H.; Sachsenhofer, R. *Macromol. Rapid Commun.* **2007**, *28*, 15. (e) Evans, R. A. *Aust. J. Chem.* **2007**, *60*, 384. (f) Williams, C. K. *Chem. Soc. Rev.* **2007**, *36*, 1573. (g) Golas, P. L.; Matyjaszewski, K. *QSAR Comb. Sci.* **2007**, *26*, 1116. (h) Spain, S. G.; Gibson, M. I.; Cameron, N. R. *J. Polym. Sci., Part A: Polym. Chem.* **2007**, *45*, 2059. (i) Barner, L.; Davis, T. P.; Stenzel, M. H.; Barner-Kowollik, C. *Macromol. Rapid Commun.* **2007**, *28*, 539. (j) Yagci, Y.; Tasdelen, M. A. *Prog. Polym. Sci.* **2006**, *31*, 1133. (k) Goodall, G. W.; Hayes, W. *Chem. Soc. Rev.* **2006**, *35*, 280. (l) Hawker, C. J.; Wooley, K. L. *Science* **2005**, *309*, 1200.

(6) (a) Fleischmann, S.; Kornber, H.; Appelhans, D.; Voit, B. I. *Macromol. Chem. Phys.* **2007**, *208*, 1050. (b) Sieczkowska, B.; Millaruelo, M.; Messerschmidt, M.; Voit, B. *Macromolecules* **2007**, *40*, 2361. (c) Thibault, R. J.; Takizawa, K.; Lowenheilm, P.; Helms, B.; Mynar, J. L.; Fréchet, J. M. J.; Hawker, C. J. *J. Am. Chem. Soc.* **2006**, *128*, 12084. (d) Slater, M.; Snauko, M.; Svec, F.; Fréchet, J. M. J. *Anal. Chem.* **2006**, *78*, 4969. (e) Malkoch, M.; Thibault, R. J.; Drockenmuller, E.; Messerschmidt, M.; Voit, B.; Russell, T. P.; Hawker, C. J. *J. Am. Chem. Soc.* **2005**, *127*, 14942. (f) Englert, B. C.; Bakbak, S.; Bunz, U. H. F. *Macromolecules* **2005**, *38*, 5868.

(7) (a) Helms, B.; Mynar, J. L.; Hawker, C. J.; Fréchet, J. M. J. *J. Am. Chem. Soc.* **2004**, *126*, 15020. (b) Mynar, J. L.; Choi, T. L.; Yoshida, M.; Kim, V.; Hawker, C. J.; Fréchet, J. M. J. *Chem. Commun.* **2005**, 5169.

(8) (a) van Steenis, D. J. V. C.; David, O. R. P.; van Strijdonck, G. P. F.; van Maarseveen, J. H.; Reek, J. N. H. *Chem. Commun.* **2005**, 4333. (b) Bakbak, S.; Leech, P. J.; Carson, B. E.; Saxena, S.; King, W. P.; Bunz, U. H. F. *Macromolecules* **2006**, *39*, 6793.

(9) Wu, P.; Feldman, A. K.; Nugent, A. K.; Hawker, C. J.; Scheel, A.; Voit, B.; Pyun, J.; Fréchet, J. M. J.; Sharpless, K. B.; Fokin, V. V. *Angew. Chem., Int. Ed.* **2004**, *43*, 3928.

(10) (a) Häussler, M.; Tang, B. Z. *Adv. Polym. Sci.* **2007**, *209*, 1. (b) Voit, B. *J. Polym. Sci., Part A: Polym. Chem.* **2005**, *43*, 2679. (c) Tomalia, D. A. *Prog. Polym. Sci.* **2005**, *30*, 294. (d) Zhi, L. J.; Wu, J. S.; Li, J. X.; Stepputat, M.; Kolb, U.; Müllen, K. *Adv. Mater.* **2005**, *17*, 1492. (e) Gao, C.; Yan, D. *Prog. Polym. Sci.* **2004**, *29*, 183. (f) Mori, H.; Muller, A. H. E. *Top. Curr. Chem.* **2003**, *228*, 1. (g) Jikei, M.; Kakimoto, M. *Prog. Polym. Sci.* **2001**, *26*, 1233. (h) Hecht, S.; Fréchet, J. M. J. *Angew. Chem., Int. Ed.* **2001**, *40*, 74. (i) Hawker, C. J. *Adv. Polym. Sci.* **1999**, *147*, 113. (j) Hult, A.; Johansson, M.; Malmstrom, E. *Adv. Polym. Sci.* **1999**, *143*, 1. (k) Morgenroth, F.; Müllen, K. *Tetrahedron* **1997**, *53*, 15349.

(11) (a) Scheel, A. J.; Komber, H.; Voit, B. *Macromol. Rapid Commun.* **2004**, *25*, 1175. (b) Smet, M.; Metten, K.; Dehaen, W. *Collect. Czech. Chem. Commun.* **2004**, *64*, 1097.

(12) For recent reviews, see: (a) Lam, J. W. Y.; Tang, B. Z. *Acc. Chem. Res.* **2005**, *38*, 745. (b) Häussler, M.; Qin, A.; Tang, B. Z. *Polymer* **2007**, *48*, 6181.

(13) Qin, A.; Jim, C. K. W.; Lu, W.; Lam, J. W. Y.; Häussler, M.; Dong, Y.; Sung, H. H. Y.; Williams, I. D.; Wong, G. K. L.; Tang, B. Z. *Macromolecules* **2007**, *40*, 2308.

(14) (a) Stolka, M.; Yanus, J.; Pai, D. *J. Phys. Chem.* **1984**, *88*, 4707. (b) Strohriegl, P.; Grazulevicius, J. V. *Adv. Mater.* **2002**, *14*, 1439. (c) Ego, C.; Grimsdale, A. C.; Weil, T.; Enkelmann, V.; Müllen, K. *Adv. Mater.* **2002**, *14*, 809. (d) He, Q. G.; Lin, H. Z.; Weng, Y. F.; Zhang, B.; Wang, Z. M.; Lei, G. T.; Wang, L. D.; Qiu, Y.; Bai, F. L. *Adv. Funct. Mater.* **2006**, *16*, 1343. (e) Deng, L.; Furuta, P. T.; Garon, S.; Li, J.; Kavulak, D.; Thompson, M. E.; Fréchet, J. M. J. *Chem. Mater.* **2006**, *18*, 386. (f) Li, Z. H.; Wong, M. S.; Fukutani, H.; Tao, Y. *Org. Lett.* **2006**, *8*, 4271. (g) Zheng, R. H.; Häussler, M.; Dong, H. C.; Lam, J. W. Y.; Tang, B. Z. *Macromolecules* **2006**, *39*, 7973.

(15) Häussler, M.; Zheng, R.; Lam, J. W. Y.; Tong, H.; Dong, H.; Tang, B. Z. *J. Phys. Chem. B* **2004**, *108*, 10645.

(16) (a) Uhrich, K. E.; Hawker, C. J.; Fréchet, J. M. J.; Turner, S. R. *Macromolecules* **1992**, *25*, 4583. (b) Muchtar, Z.; Schappacher, M.; Deffieux, A. *Macromolecules* **2001**, *34*, 7595. (c) Grayson, S. M.; Fréchet, J. M. J. *Macromolecules* **2001**, *34*, 6542. (d) Xu, K.; Peng, H.; Sun, Q.; Dong, Y.; Salhi, F.; Luo, J.; Chen, J.; Huang, Y.; Xu, Z.; Tang, B. Z. *Macromolecules* **2002**, *35*, 5821.

(17) Malkoch, M.; Schleicher, K.; Drockenmuller, E.; Hawker, C. J.; Russell, T. P.; Wu, P.; Fokin, V. V. *Macromolecules* **2005**, *38*, 3663.

(18) (a) Oshima, N.; Suzuki, H.; Moro-oka, Y. *Chem. Lett.* **1984**, 1161. (b) Tilley, T. D.; Grubbs, R. H.; Bercaw, J. E. *Organometallics* **1984**, *3*, 274. (c) Rasmussen, L. K.; Boren, B. C.; Fokin, V. V. *Org. Lett.* **2007**, *9*, 5337.

(19) Chan, T. R.; Hilgraf, R.; Sharpless, K. B.; Fokin, V. V. *Org. Lett.* **2004**, *6*, 2853.

(20) (a) Hawker, C. J.; Lee, R.; Fréchet, J. M. J. *J. Am. Chem. Soc.* **1991**, *113*, 4583. (b) Frey, H.; Hölter, D. *Acta Polym.* **1999**, *50*, 67.

(21) Young, R. J.; Lovell, P. A. *Introduction to Polymers*, 2nd ed.; Chapman & Hall: London, 1991.

(22) (a) Yan, D. Y.; Muller, A. H. E.; Matyjaszewski, K. *Macromolecules* **1997**, *30*, 7024. (b) Ishizu, K.; Tsubaki, K.; Mori, A.; Uchida, S. *Prog. Polym. Sci.* **2003**, *28*, 27. (c) Grebel-Koehler, D.; Liu, D. J.; De Feyter, S.; Enkelmann, V.; Weil, T.; Engels, C.; Samyn, C.; Müllen, K.; De Schryver, F. C. *Macromolecules* **2003**, *36*, 578.

(23) Liu, J.; Zheng, R.; Tang, Y.; Haussler, M.; Lam, J. W. Y.; Qin, A.; Ye, M.; Hong, Y.; Gao, P.; Tang, B. Z. *Macromolecules* **2007**, *40*, 7473.

(24) Dong, H. C.; Zheng, R. H.; Lam, J. W. Y.; Häussler, M.; Qin, A. J.; Tang, B. Z. *Macromolecules* **2005**, *38*, 6382.

(25) Wu, L.; Tong, W. Y. Y.; Zhong, Y.; Wong, K. S.; Hua, J.; Häussler, M.; Lam, J. W. Y.; Tang, B. Z. *Appl. Phys. Lett.* **2006**, *89*, 191109.

(26) (a) Campbell, L.; Sharp, D. N.; Harrison, M. T.; Denning, R. G.; Turberfield, A. J. *Nature (London)* **2000**, *404*, 53. (b) Kim, J. M. *Macromol. Rapid Commun.* **2007**, *28*, 1191.

(27) (a) Yuan, W. Z.; Qin, A. J.; Lam, J. W. Y.; Sun, J. Z.; Dong, Y. Q.; Häussler, M.; Liu, J. Z.; Xu, H. P.; Zheng, Q.; Tang, B. Z. *Macromolecules* **2007**, *40*, 3159. (b) Hua, J. L.; Lam, J. W. Y.; Dong, H. C.; Wu, L. J.; Wong, K. S.; Tang, B. Z. *Polymer* **2006**, *47*, 18. (c) Lam, J. W. Y.; Qin, A. J.; Dong, Y. P.; Lai, L. M.; Häussler, M.; Dong, Y. Q.; Tang, B. Z. *J. Phys. Chem. B* **2006**, *110*, 21613.

(28) (a) Kingslake, R. *Optics in Photography*; SPIE Optical Engineering Press: Bellingham, WA, 1992. (b) Pedrotti, L. S.; Pedrotti, F. L. *Optics and Vision*; Prentice Hall: Upper Saddle River, NJ, 1998.

(29) (a) Smith, F. G.; King, T. A.; Wilkins, D. *Optics and Photonics: an Introduction*, 2nd ed.; Wiley: Hoboken, NJ, 2007. (b) Sharma, K. K. *Optics: Principles and Applications*; Academic Press: Amsterdam, 2006.

(30) (a) Singh, P. N. D.; Mandel, S. M.; Sankaranarayanan, J.; Muthukrishnan, S.; Chang, M.; Robinson, R. M.; Lahti, P. M.; Ault, B. S.; Gudmundsdottir, A. D. *J. Am. Chem. Soc.* **2007**, *129*, 16263. (b) Li, Z.; Dong, Y.; Haussler, M.; Lam, J. W. Y.; Dong, Y.; Wu, L.; Wong, K. S.; Tang, B. Z. *J. Phys. Chem. B* **2006**, *110*, 2302. (c) Bräse, S.; Gil, C.; Knepper, K.; Zimmermann, V. *Angew. Chem., Int. Ed.* **2005**, *44*, 5188. (d) Jia, J. P.; Baker, G. L. *J. Polym. Sci., Part B: Polym. Phys.* **1998**, *36*, 959.

MA800538M